



RIVERSIDE RESEARCH INSTITUTE



330 West 42nd Street / New York, New York 10036 / (212) 563-4545

23 November 1992

TECHNICAL REPORT TR-1/C68-603B

TREND FIELD TEST REPORT

DTIC
ELECTE
DEC 9 1992
S C D

This Report is submitted in compliance with
CDRL Seq. No. A002, Item 002AE-Task 3B
under Contract No. N00014-91-C-0015

92-30349
56pk

DISTRIBUTION STATEMENT A

Approved for public release
Distribution Unlimited

Prepared for:
Naval Air Warfare Center
Aircraft Division
P.O. Box 5152
Warminster, PA 18974-0591
Att: Mr. Tom Pohle, 5011/Mr. Mike Hess, 5014

"THIS PROPOSAL INCLUDES DATA THAT SHALL NOT BE DISCLOSED OUTSIDE THE GOVERNMENT AND SHALL NOT BE DUPLICATED, USED, OR DISCLOSED IN WHOLE OR IN PART FOR ANY PURPOSE OTHER THAN TO EVALUATE THE PROPOSAL. IF, HOWEVER, CONTRACT IS AWARDED TO THIS OFFEROR AS A RESULT OF, OR IN CONNECTION WITH, THE SUBMISSION OF THIS DATA, THE GOVERNMENT SHALL HAVE THE RIGHT TO DUPLICATE, USE, OR DISCLOSE THE DATA TO THE EXTENT PROVIDED IN THE CONTRACT. THIS RESTRICTION DOES NOT LIMIT THE GOVERNMENT'S RIGHT TO USE INFORMATION CONTAINED IN THE DATA IF IT IS OBTAINED FROM ANOTHER SOURCE WITHOUT RESTRICTION. THE DATA SUBJECT TO THIS RESTRICTION ARE AS MARKED."

RIVERSIDE RESEARCH INSTITUTE

TABLE OF CONTENTS

TEST REPORT	1
REFERENCES	11
APPENDIX A - SYSTEM SCHEMATIC, OPTICAL DIMENSIONS, & PHOTOGRAPH	12
APPENDIX B - LIST OF DIGITIZED DATA FILES	16
APPENDIX C - DIGITIZED DATA FILE/SPECTRUM ANALYZER PLOT CROSS REFERENCE	22
APPENDIX D - WEATHER CONDITIONS	24
APPENDIX E - SPECTRUM ANALYZER PLOTS & SAMPLE DIGITIZED PLOT	26

DTIC QUALITY INSPECTED 2,

St-A per telecon, Dr. Watcher,
ONR/ Arlington, VA 22217.

JK 12-9-92

Accession For	
NTIS ORIS	<input checked="" type="checkbox"/>
DTIC TAB	<input type="checkbox"/>
Unannounced	<input type="checkbox"/>
Justification	
By	
Distribution/	
Availability Codes	
Dist	Avail and/or Special
A-1	

RIVERSIDE RESEARCH INSTITUTE

INTRODUCTION

The following report describes work carried out, leading up to and including the final ground based field test of the Testbed for Realistic Evaluation of Novel Discriminants (TREND) electro-optical system. The ultimate goal of this system is to provide a means of passive discrimination between moving objects and a stationary cluttered background by virtue of signal source angular velocity separation. Angular velocity may be inferred by signal frequency on a single periodically masked detector as the source moves across its field of view. The signal amplitude must vary sufficiently over an angular subtense equal to half the mask period to register above the local noise. Such signals may arise from point objects (with respect to half the mask period) or hard edges perpendicular to the mask period.

An additional twist to this method, utilized in the TREND sensor, optically filters selected spatial frequencies by dividing the wavefront at the aperture, transmitting radiation through a double slit. If spatial coherence is maintained over the entrance aperture a periodic interference pattern is formed which when properly matched to the mask period will exhibit a periodic signal similar to that produced with an undivided wavefront. The advantage to this scheme is that spatial filtering is performed optically. The obvious disadvantage is reduction of received energy. The current TREND system uses a scanning sensor to simulate moving radiation sources with an actually stationary background, thus the background source signals will be modulated at the nominal frequency proportional to the scanning angular velocity.

The ground based field test effectively demonstrated the theoretical signal modulation (under controlled conditions), yet system noise and lack of detector sensitivity prohibited the collection of sufficiently strong signals from the natural environment. The field testing was conducted at the Naval Air Warfare Center (NAWC) in Warminster, PA from June 22, 1992 to June 24, 1992. The sensor was mounted in a third story room, scanning horizontally over a parking lot and airfield (appendix A, figure 3). The design periodic signal was observed while scanning an artificial blackbody source at 206 meters; no such signal was observed while scanning a welding torch at 1536 meters.

DOUBLE SLIT INDUCED INTERFERENCE

The novelty of the TREND sensor stems in its use wavefront division to alter the MTF of the optical system such that it acts as a spatial filter. The detector mask is used to translate angular velocity information to the time domain for display, recording, and discrimination purposes.

A useful interferometric model treats the TREND aperture as the classic Young's double slit illuminated by a plane wave. Interference of the wavefronts produces an intensity distribution proportional to the cosine of the phase difference between each wavefront. As seen in figure 1,

RIVERSIDE RESEARCH INSTITUTE

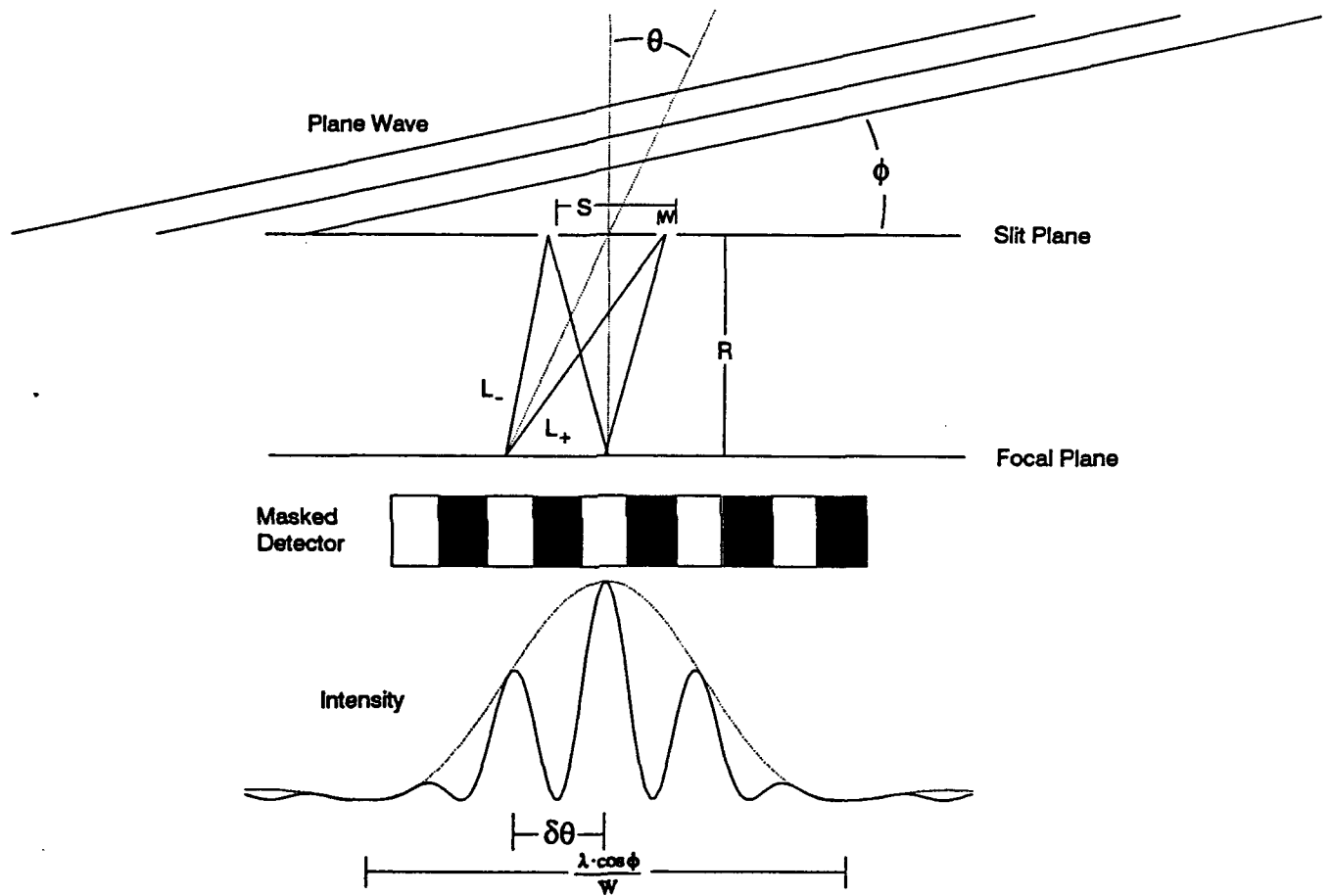


Figure 1. Fringe Model

RIVERSIDE RESEARCH INSTITUTE

the angular separation, $\delta\theta$, between fringes is $\lambda/s \cdot \cos\phi/\cos\theta \cdot \sqrt{1 + (s/2R)^2}$, where λ is the wavelength of light, s is the center to center separation of the slits, θ is the fringe observation angle with respect to the slit plane, ϕ is the plane wave incident angle with respect to the slit plane, and R is the range at which the pattern is observed (in our case the focal length of the imaging optics). Note that the entire focal length of the system is not used since the wavefront is divided between the afocal telescopic optics and imaging optics. The schematic figure 1 shows the fringe pattern modulated by the point spread function of a single slit of width w . Most of the energy is contained within the angular subtense $\lambda/w \cdot \cos\phi$. Figure 1 also shows a portion of a single detector masked at the appropriate spatial frequency to give maximum signal modulation as the fringe pattern moves across its field of view. The modulation occurs at a frequency equal to the source angular velocity divided by the detector mask angular subtense.

The following provides a simple model for fringe separation with respect to design parameters. Referring to figure 1 we see that the path difference, PD, from the center of each slit to the focal plane is given by

$$PD = L_+ - L_-$$

When $\frac{\partial PD}{\partial \theta} \cdot \delta\theta = \lambda \cdot \cos\phi$ consecutive intensity maxima are observed.

Since

$$L_{\pm} = R\sqrt{1 + (\sin\theta \pm s/2R)^2}$$

$$\frac{\partial L_{\pm}}{\partial \theta} = \frac{R \cos\theta (\sin\theta \pm s/2R)}{\sqrt{1 + (\sin\theta \pm s/2R)^2}}$$

therefore

$$\frac{\partial PD}{\partial \theta} = \frac{R \cos\theta (\sin\theta + s/2R)}{\sqrt{1 + (\sin\theta + s/2R)^2}} - \frac{R \cos\theta (\sin\theta - s/2R)}{\sqrt{1 + (\sin\theta - s/2R)^2}}$$

Close to the center of the field $\sin\theta \ll s/2R$, so

$$\frac{\partial PD}{\partial \theta} = \frac{s \cdot \cos\theta}{\sqrt{1 + (s/2R)^2}}$$

and

$$\delta\theta = \frac{\lambda \cdot \cos\phi}{\frac{\partial PD}{\partial \theta}} = \frac{\lambda \cdot \cos\phi \sqrt{1 + (s/2R)^2}}{s \cdot \cos\theta}$$

Available fringe contrast may be maximized by minimizing the ratio of the sum of the partial differentials of the fringe separation with respect to each design parameter (i.e., λ , s , ϕ , w , $f1$) to the fringe separation. Stated mathematically the relative fringe shift (RFS) is,

RIVERSIDE RESEARCH INSTITUTE

$$RFS = \sum_{i=1}^n \frac{\partial \delta \theta}{\partial x_i} \cdot \frac{\delta x_i}{\delta \theta}$$

where the elements, i , are given as follows:

$$\lambda \rightarrow \frac{\delta \lambda}{\lambda}$$

$$s \rightarrow \frac{-\delta s}{s[1 + (\frac{s}{2R})^2]}$$

$$\phi \rightarrow \frac{\delta \phi \tan \phi}{1 + (\frac{s}{2R})^2}$$

$$R \rightarrow \frac{-\left(\frac{s}{2R}\right)^2 \delta R}{R[1 + (\frac{s}{2R})^2]}$$

Note that $\delta \lambda$ is limited by the optical filter bandwidth, δs is limited to the slit width, $\delta \phi$ represents a shift in the effective plane wave incident angle and δR represents a shift in the detector plane from the design focal plane.

ATMOSPHERIC TURBULENCE

As mentioned previously, interference fringes will be produced if the wavefront approximates a plane wave at the entrance aperture. This coherent area is usually quantified in terms of the coherence diameter, r_0 . This is a function of atmospheric turbulence, the path length over which the radiation travels, and the wavelength of light. It is given by formula as follows:

$$r_0 = (0.4233 C_n^2 k^2 L)^{-3/5}$$

where:

$$\begin{aligned} C_n^2 &= \text{refractive index structure parameter} \\ k &= \text{radiation wavenumber} \\ L &= \text{path length.} \end{aligned}$$

We did not measure the coherence diameter during the field test, but may estimate it based upon typical values of C_n^2 [1]. Close to the ground, the refractive index structure parameter is highly dependent upon the time of day and type of surface over which it is

RIVERSIDE RESEARCH INSTITUTE

measured. Generally the value is proportional to the degree of thermal equilibrium between the surface and the atmosphere. Using bounding values of C_n^2 one may estimate reasonable coherence diameters. These are shown for various ranges in table 1.

Table 1

L (m)	r_0 (m) for C_n^2 ($m^{-2/3}$)	
	1.5×10^{-12}	1.5×10^{-14}
1	21	330
100	1.3	21
206	0.90	14
1000	0.34	5.3
1536	0.26	4.0

OPTICAL MTF

The aperture is divided to alter the MTF (modulation transfer function) such that undesired spatial frequencies are filtered out. In general, the MTF of an optical system (in cycles/radian) is the autocorrelation function of the entrance pupil divided by the admitted radiation wavelength. The slit pupil patterns used in the TREND system increase the high to low frequency MTF ratio with respect to that of a non-divided pupil, while maintaining the same absolute MTF at high frequency. A simple comparison of full aperture and slit aperture MTFs can be made by approximating the apertures as rectangular. These theoretical MTFs are graphed in figure 2, normalized to the full aperture. The actual TREND MTFs will differ slightly because those shown assume rectangular pupils and diffraction limited optics. The signal available at any frequency is proportional to the product of the admitted energy and the optical MTF. Given equal irradiances at the entrance aperture, the admitted energy is proportional to the pupil area. At spatial frequencies greater than the design frequency ($f = s/\lambda$) the slit pupil signal will be modified by the pupil area reduction, while at lower frequencies, modified by the product of the MTF and pupil area reductions.

PRELIMINARY LABORATORY TESTING¹

Prior to performing the ground based field test the system was tested in the laboratory with a soldering iron source and vertical slit aperture measuring 5×10^{-3} by 2.5×10^{-5} radians.

¹ All laboratory testing performed at chip carrier temperature equal to 80 K. Field testing was performed at 70 K.

RIVERSIDE RESEARCH INSTITUTE

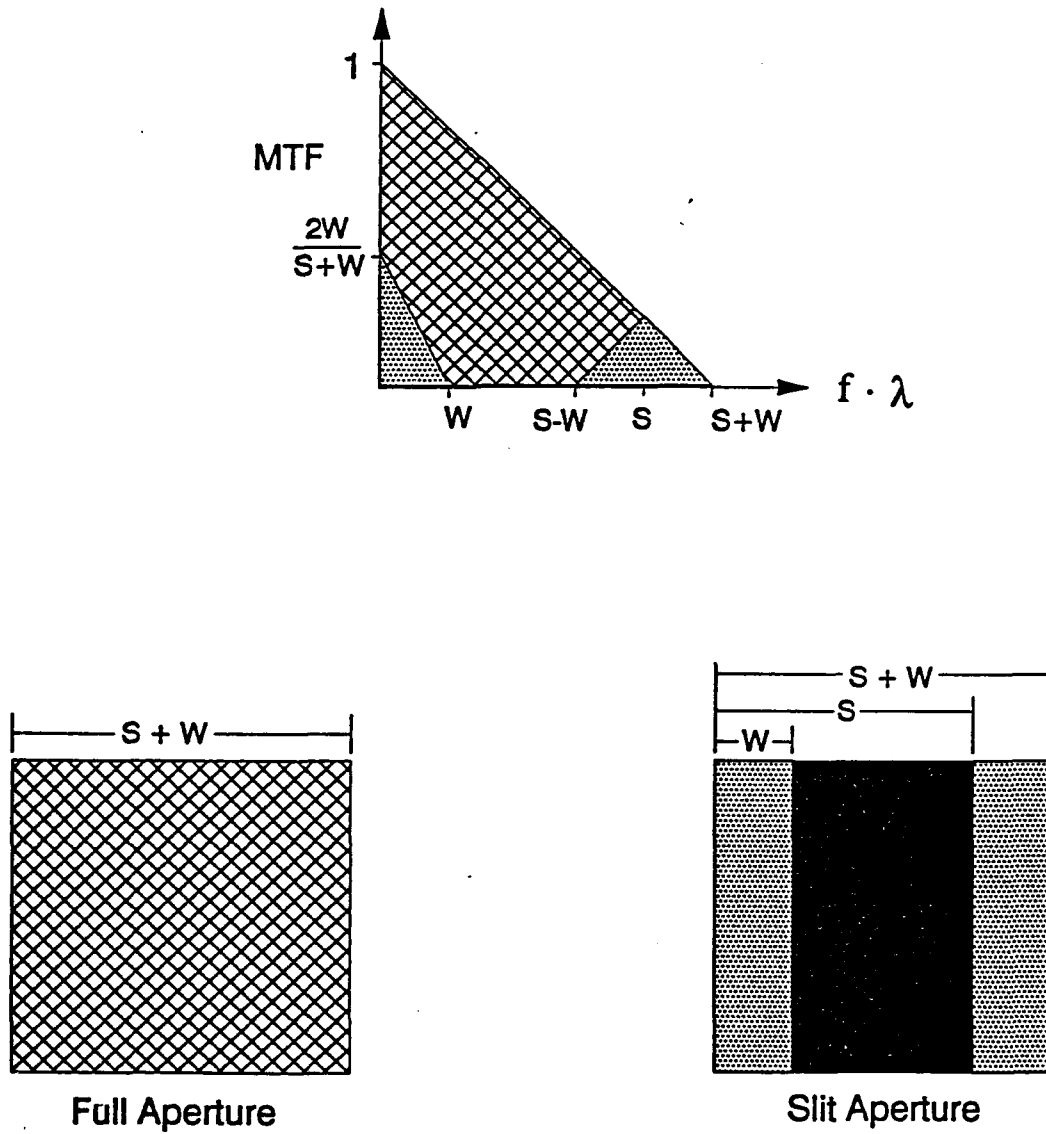


Figure 2. Theoretical MTF

RIVERSIDE RESEARCH INSTITUTE

The iron temperature was 593 K, measured with a thermocouple. Preamplifiers were set at 10^6 volts/amp gain.² With the scanner stationary the radiation was chopped at 20 Hz just prior to the slit pupil. Signal and noise data was recorded for various pupil and detector element combinations as shown in table 2.

Table 2

FILTER 2		PUPIL 2		
PUPIL	SIGNAL (mV)	FILTER	SIGNAL (mV)	NOISE (mV @ 120 Hz)
1	80	0	120	20
2	100	1	10	20
3	160	2	100	20
4	580	3	10	20
5	580	4	55	20
6	580	5	--	100
		6	20	40
		7	20	40

Additionally, with pupil 2 (appendix A, figure 2) inserted, the detectors were scanned across the source at five speeds ranging from 2×10^{-3} to 2×10^{-4} radians/second. Data was digitized and recorded on disk from eight multiplexed channels. A list of those data files is shown in appendix B.

NOISE CONSIDERATIONS

In general the system was found to be very noisy, predominated by the fundamental 60 Hz line frequency and multiples. Testing in the laboratory using the dual trace oscilloscope as a differential amplifier proved that the noise was common to both the detector ground and signal leads. Inputting a detector signal lead directly to the oscilloscope without grounding the detector to chassis gave a 1.5 volt signal at 60 Hz. Grounding the detector to chassis reduced this to 5 millivolts random frequency. This was analogous to the normal operating condition, except that the oscilloscope provided voltage to voltage amplification while the preamplifiers provided current to voltage amplification. Under normal operating conditions noise was reduced to a minimum of 20 millivolts at 120 Hz after passing through the Texas Instruments (TI) filter circuit (low pass 60 Hz notch filter, -3 dB at 20 Hz). More typical noise values ranged up to 100 millivolts. The greatest noise reduction was obtained by bringing the detector ground and signal

² Over the course of the field testing the preamplifiers gains were set at 10^5 or 10^6 volts/amp since system noise would cause saturation at higher values.

RIVERSIDE RESEARCH INSTITUTE

leads to two channels of the oscilloscope, then inverting one channel. This differential amplifier configuration gave a random output voltage of 2 millivolts.

Generally each preamplifier showed a DC offset around 400 millivolts, the exception being number 10 with an offset of 70 millivolts. Preamplifier 10 outputs were the noisiest.

Common mode noise predominates in the TREND system because the preamplifiers use single ended inputs; the non-inverting input is carried by the coaxial signal line shield (appendix A, figure 1). Due to multiple grounding of the shield (at both the dewar and amplifier box) a current flows between these points which couples with the real signal current. The problem is further magnified by capacitive coupling between 22 unused detector lead coaxial cables and a noisy laboratory environment since the shields are all connected to the dewar ground point [3]. This is evidenced by noise changing by an order of magnitude as a person moves around the room or adjusts the cable positions. Scanning operation gives rise to continually changing noise values. Proper grounding and shielding employs biaxial or triaxial cables to bring the signal ground and detector leads to the amplifiers, and grounding of the entire shield (dewar, cable, and preamplifier box) only at the dewar [4]. The signal ground lead should be attached between the dewar ground point and the preamplifier non-inverting input. The detector output should be attached to the preamplifier inverting input. Ideally each detector should have both output and ground leads; however, the TREND chip carrier uses a common ground for all 32 detectors. This common signal ground should be buffered before splitting to the non-inverting inputs of each preamplifiers [5].

A further refinement reduces the effect of common mode noise produced by leakage through the shield by placing a resistor of equal magnitude to that of the feedback resistor in series with the non-inverting amplifier input and signal ground point [6].

FIELD TEST

The ground based field test was conducted from a third story room in the NAWC facility with the sensor 14 meters above the ground scanning at 1.57×10^{-3} radians/second out toward the eastern horizon. Unobscured line of sight scan could be obtained for -45 to +45 degrees in azimuth and -10 to +30 degrees in elevation. Due to system noise the preamplifiers saturated at high gain so full detector sensitivity was unavailable. An artificial blackbody source of 1.75×10^{-2} meter diameter at 206 meters range was scanned successfully at temperatures 375 C, 500 C, and 600 C. A welding torch (assumed temperature 1700 C) at 1536 meters range did not produce an observable signal (see Energy Considerations for justification). A map indicating sensor and source positions is shown in figure 3. We observed one case of frequency modulation with a full aperture pupil when the sensor was not scanning. We assume sensor or turbulence induced wavefront jitter caused these signals.

ENERGY CONSIDERATIONS

The noise equivalent input (NEI) of the system is the contrast irradiance at the TREND aperture which will produce a signal to noise ratio of unity. This is used to quantify sensitivity.

RIVERSIDE RESEARCH INSTITUTE

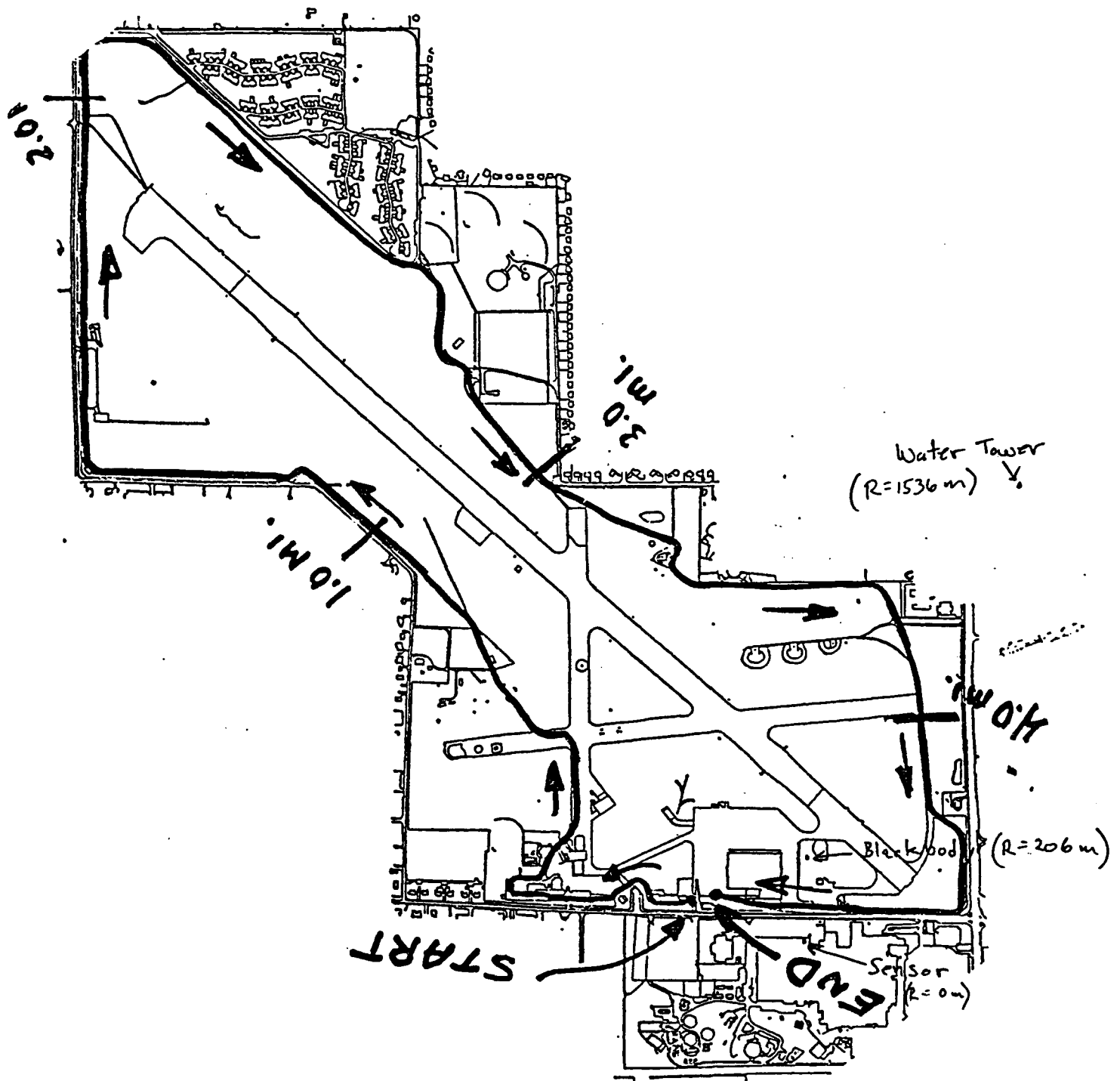


Figure 3. Source - Sensor Geometry

RIVERSIDE RESEARCH INSTITUTE

For a subpixel source it may be calculated as follows:

$$CE(A, R, T, \Delta \lambda) = \frac{A \cdot \tau(R) \cdot [L(\Delta \lambda, T_{\text{source}}) - L(\Delta \lambda, T_{\text{back}})]}{R^2}$$

where:

CE	=	contrast irradiance
A	=	area of the source
R	=	range to the source
$\tau(R)$	=	atmospheric transmission over range R
L	=	radiance
T	=	absolute temperature
$\Delta \lambda$	=	waveband

We calculated the contrast irradiance at the sensor for three different blackbody source temperatures. The atmospheric transmission was assumed to be unity over the dewar window spectral transmission band (1 micron width centered on 10 microns) [6]. Voltage measurements were taken via oscilloscope from TI channel 3 with preamplifier gain set to 10^6 volts/amp and chopping frequency at 25 Hz. Table 3 shows the contrast irradiances, signal voltages, and resultant noise equivalent inputs. In all cases the noise was 100 millivolts.

Table 3

TEMPERATURE (K)	CE (w/m^2)	SIGNAL (V)	NEI (w/m^2)
873	9.27×10^{-7}	1.50	6.17×10^{-8}
773	7.08×10^{-7}	1.25	5.65×10^{-8}
648	4.58×10^{-7}	0.76	6.02×10^{-8}

Note that these NEIs were measured with a full aperture pupil. Slit pupil apertures increase these values by factors ranging from 2.6 to 5.0 (appendix A, figure 2).

Since we did not observe the expected modulated signal from the welding torch³ (a very hot source), we calculated its contrast irradiance at the sensor. The resultant value ($1.7 \times 10^{-7} \text{ w}/\text{m}^2$) is close enough to the NEI to justify the experimental results.

³ Assumptions - hot area = 4 cm^2 , temperature = 1973 K [7], atmospheric transmission = 1 (worst case 0.5) [8].

RIVERSIDE RESEARCH INSTITUTE

REFERENCES

- [1] W. Wolfe, G. Zissis, "The Infrared Handbook," Environmental Research Institute of Michigan, (1985) pp. 6-11 - 6-14.
- [2] R. Morrison, "Grounding and Shielding Techniques in Instrumentation," 3rd Edition, Wiley, New York, (1986) p. 145, 148.
- [3] P. Horowitz, W. Hill, "The Art of Electronics," Cambridge University Press, Cambridge, (1980) p. 308.
- [4] Ref. [2] pp. 37 - 54.
- [5] Ref. [3] p. 311.
- [6] Ref. [3] p. 113.
- [7] D. Lide, "CRC Handbook of Chemistry and Physics," 72nd Edition, CRC Press, Boca Raton, (1991) p. 12-136.
- [8] "Electro-Optics Handbook, " 2nd Edition, RCA Commercial Engineering, Harrison, NJ, (1974) pp. 98 - 100.

RIVERSIDE RESEARCH INSTITUTE

APPENDIX A

RIVERSIDE RESEARCH INSTITUTE

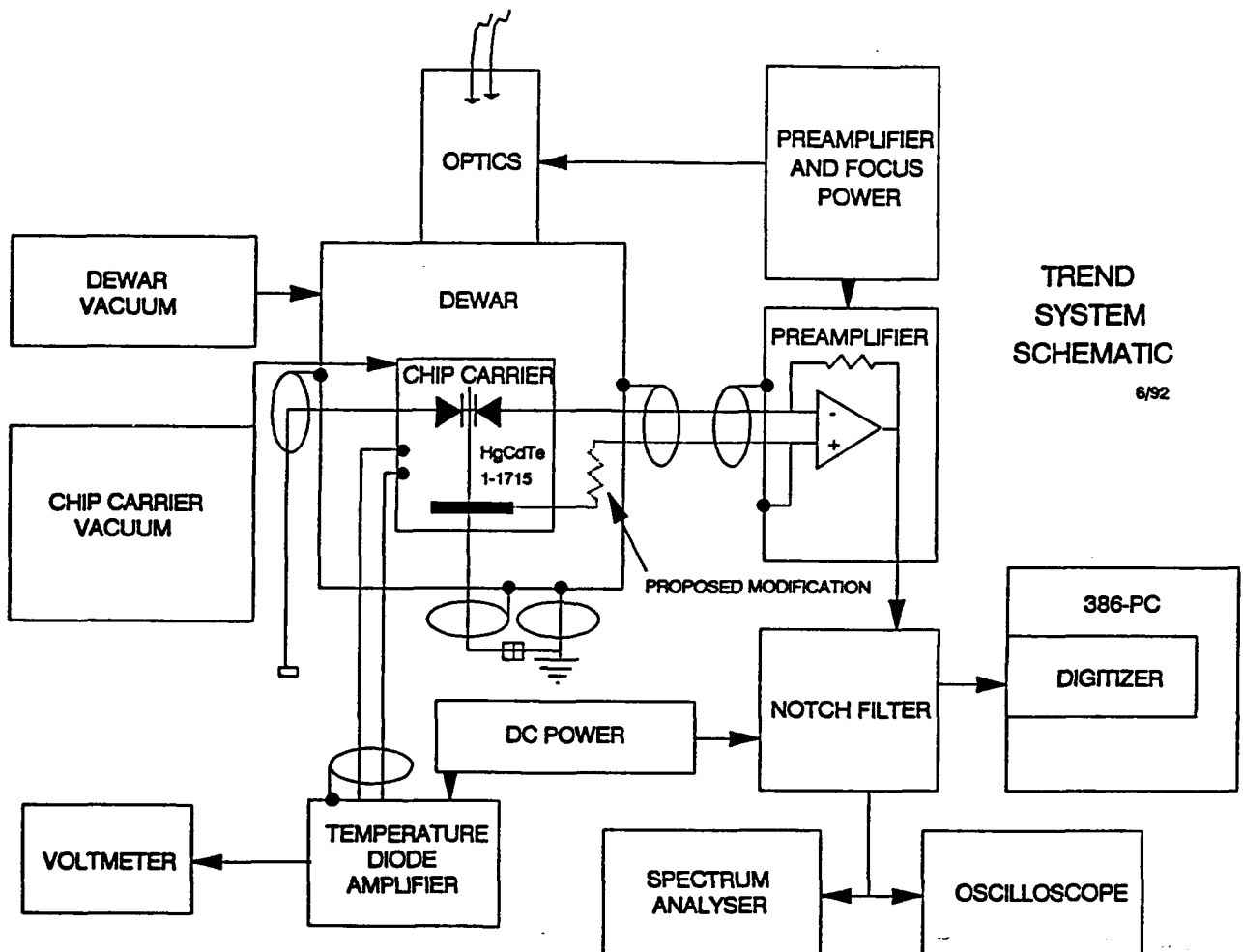
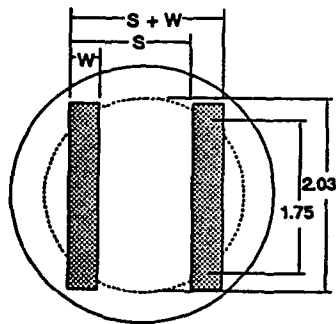
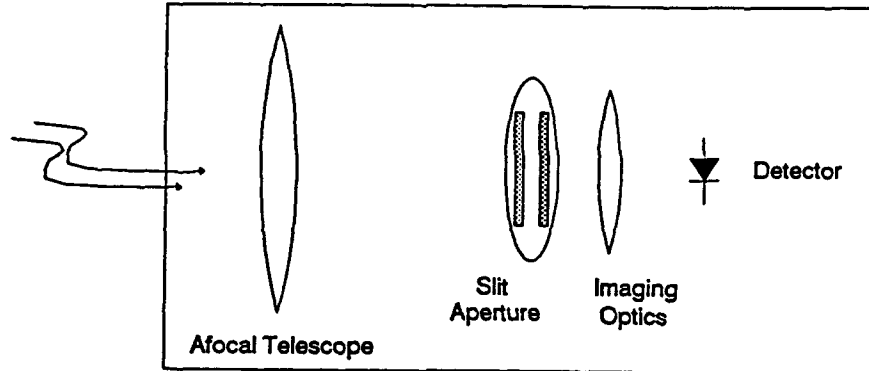


Figure 1. System Schematic

RIVERSIDE RESEARCH INSTITUTE

Optical Layout- Entrance pupil = 20.3 cm, $f/\# = 2.13$

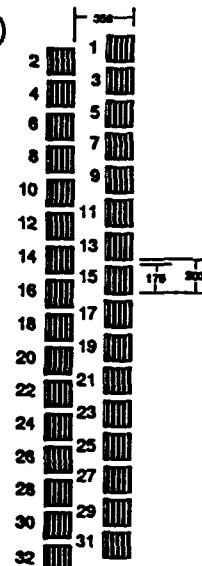
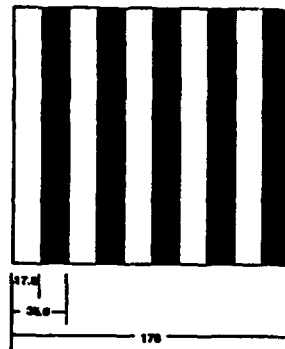


Pupil Dimensions (cm)

Pupil	S	W	S/W	R
1	1.049	0.183	5.77	0.20
2	1.049	0.239	4.36	0.26
3	1.044	0.348	3.00	0.38

$R = \text{slit pupil area} / \text{circular pupil area}$

Detector Plane Dimensions (microns)



Typical $D^* = 1.34 \times 10^{11} \text{ cm Hz}^{1/2}/\text{W}$, chip carrier # 1-1715
Temp sensor on chip carrier, -1.7 mV/K, 0.680 V @ 300K

Figure 2. Optical Dimensions

RIVERSIDE RESEARCH INSTITUTE

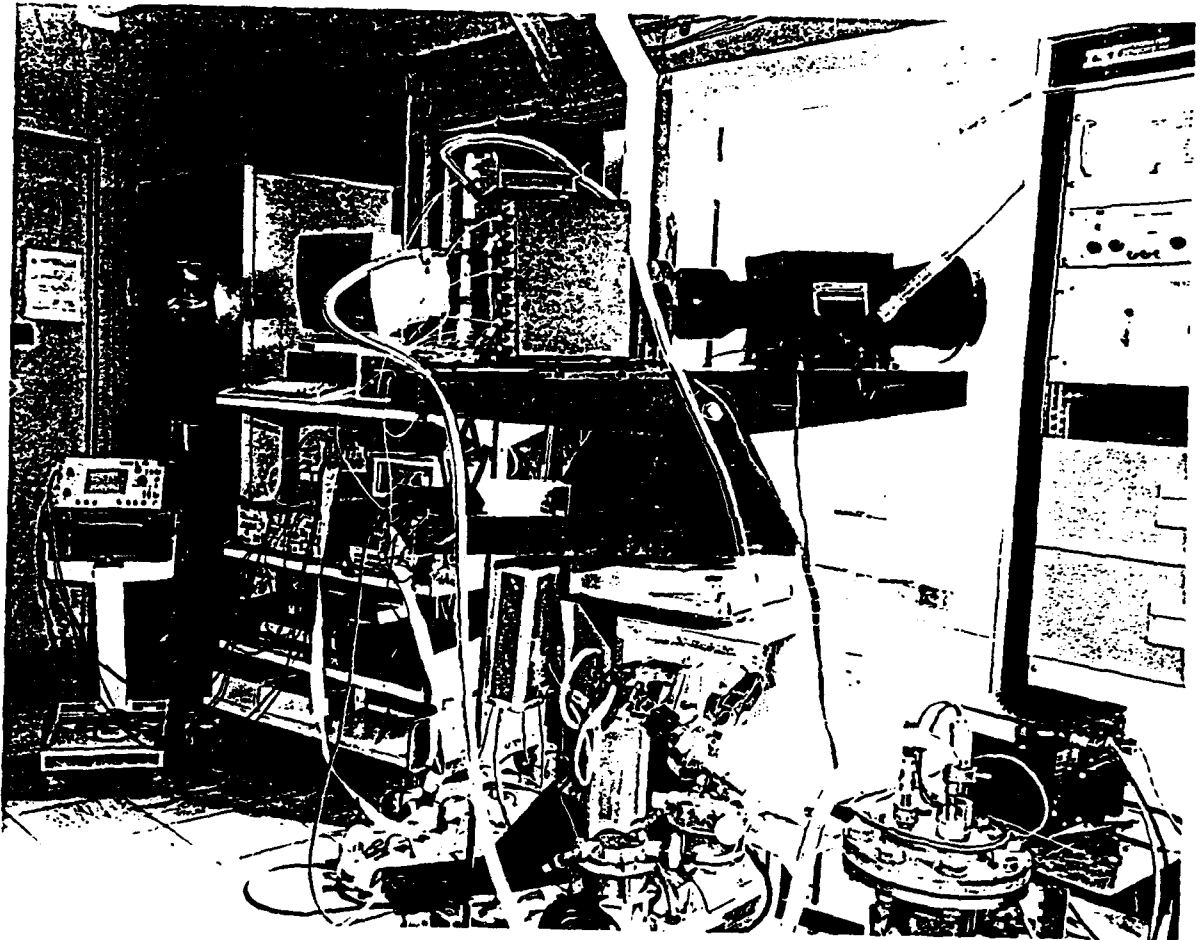


Figure 3. Photograph of TREND System

RIVERSIDE RESEARCH INSTITUTE

APPENDIX B

RIVERSIDE RESEARCH INSTITUTE

DATA COLLECTION

The spectrum analyzer plots represent the output of TI channel 3, lowpass filtered by the spectrum analyzer with a cutoff at 100 Hz.

The digitized data files represent 15 seconds of raw data from TI channels 0, 1, 2, 3, 4, 5, 6, 7, time sampled at 128 Hz. The 4 seconds shown on the spectrum analyzer plots are located somewhere within this time frame, typically after the 5 seconds of pretrigger data.

The following Labtech Notebook icon-generated software block files drive the Metrabyte DASH-16 digitizer board:

- a. TRIG8 - Digitize, time stamp, display, store channels 0 - 7.
- b. SCANODD - Digitize, display channels 1, 3, 5, 7.
- c. SCANEVEN - Digitize, display channels 0, 2, 4, 6.
- d. SCAN03 - Digitize, display channels 0, 1, 2, 3.
- e. SCAN47 - Digitize, display channels 4, 5, 6, 7.
- f. AVETEST - Replay channel 0 with various averaging schemes (0 - 10 sec).
- g. EVEN - Replay channels 0, 2, 4, 6 (0 - 10 sec).
- h. ODD - Replay channels 1, 3, 5, 7 (0 - 10 sec).
- i. REPLAY3 - Replay channel 3 (0 - 15 sec).

RIVERSIDE RESEARCH INSTITUTE

DIGITIZED DATA FILES

base#, basx# - 6/22/92

basy# - 6/23/92

basz# - 6/24/92

FILE	PUPIL	GAIN (V/A)	SCAN (deg/s)	COMMENT
base1	6	10^5	0.038	water tower/welder
base2	2			water tower/no welder
basx0				water tower/no welder
basx1				trees at 1 km
basx2				aperture covered
basx3				aperture covered
basx4				water tower/welder
basx5				water tower/welder
basx6				water tower/welder
basx7				water tower/welder
basx8				water tower/welder
basx9				water tower/welder
basx10		10^6		water tower/welder
basx11			0.025	water tower/welder
basx12			0.019	water tower/welder
basx13				water tower/welder
basx14				crane cable at water tower
basx15				crane cable at water tower
basx16				cloud along horizontal edge
basx17				cloud along vertical edge
basx18				cloud along vertical edge
basx19				nearby cloud
basx20				tree tops at 1 km

RIVERSIDE RESEARCH INSTITUTE

FILE	PUPIL	GAIN (V/A)	SCAN (deg/s)	COMMENT
basx21	2	10 ⁶	0.093	water tower/welder
basx22				water tower/no welder
basx23				aperture covered partially
basx24				aperture covered
basx25				aperture covered, person moving
basx26				aperture covered then uncovered
basx27				clouds
basx28			0.087	crane cable at water tower
basx29				water tower/welder
basx30				water tower/no welder, trees
basx31				plane w/props moving at 200 m
basx32				tarmac at 200 m
basx33				?
basx34			?	?
basx35				water tower/no welder
basx36				water tower/no welder
basx37				water tower/welder
basy0	2	10 ⁶	?	?
basy1			0.000	aperture covered
basy2				aperture open
basy3				aperture covered
basy4			0.093	crane cable and crane at tower
basy5				tree tops at 1 km
basy6				?
basy7				?
basy8				?
basy9				?

RIVERSIDE RESEARCH INSTITUTE

FILE	PUPIL	GAIN (V/A)	SCAN (deg/s)	COMMENT
basy10	2	10 ⁶	0.093	?
basy11				?
basy12	4			1.35 cm diameter, 600 C BB @ 206 m
basy13	2			1.35 cm diameter, 600 C BB @ 206 m
basy14				1.35 cm diameter, 600 C BB @ 206 m
basy15				?
basy16	3			1.35 cm diameter, 600 C BB @ 206 m
basy17	2			1.35 cm diameter, 600 C BB @ 206 m
basy18				1.35 cm diameter, 600 C BB @ 206 m
basy19	1			1.35 cm diameter, 600 C BB @ 206 m
basy20				1.35 cm diameter, 600 C BB @ 206 m
basy21	3			1.35 cm diameter, 500 C BB @ 206 m
basy22	4			1.35 cm diameter, 500 C BB @ 206 m
basy23				1.35 cm diameter, 500 C BB @ 206 m
basy24			0.000	grass background at 206 m
basy25				grass background at 206 m
basy26			0.093	crane wire at tower
basy27			0.093	1.35 cm diameter, 375 C BB @ 206 m
basy28				?
basy29	3		0.093	1.35 cm diameter, 375 C BB @ 206 m
basy30				1.35 cm diameter, 375 C BB @ 206 m
basy31				1.35 cm diameter, 375 C BB @ 206 m
basy32				clouds
basz0	2		0.000	covered aperture, typical noise
basz1				covered, typical spikes
basz2			0.093	building at about 200 m
basz3				covered aperture

RIVERSIDE RESEARCH INSTITUTE

FILE	PUPIL	GAIN (V/A)	SCAN (deg/s)	COMMENT
basz4	2	10^6	0.093	uncommonly noisy scan
basz5				uncommonly noisless scan
basz6				cumulous clouds, 1-2 km
basz7				30 Hz signal when scanner -20 degrees azimuth, cumulous clouds 1-2 km range, repeatable w.r.t. scanner position, not cloud position
basz8-20				not noteworthy
scan0			6.123	320 C, 5×10^{-3} by 2.5×10^{-5} radian source at focal point of 3.05 meter collimater
scan1			0.048	
scan2			0.031	
scan3			0.019	
scan4			0.014	

RIVERSIDE RESEARCH INSTITUTE

APPENDIX C

RIVERSIDE RESEARCH INSTITUTE

DATA-FILE - SPECTRUM ANALYZER PLOT CROSS REFERENCE

Spectrum Analyzer Plot

Digitized Data File

1	basyl2
2	basyl30
3	basyl31
4	basyl32
5	basyl24
6	basyl27
7	basyl29
8	basyl21
9	basyl18
10	typical of basyl19,20
11	basyl17
12	basyl16
13	none, typical transient with aperture covered
14	basyl23
15	basyl25
16	none, typical noise spike
17	typical of basz5, 6
18	basz7
19	basz4
20	none, relatively low noise
21	basz5 ?
22	basz6 ?
23	basz5 ?
24	basz4
25	basz0
26	basz1

WIRING CROSS REFERENCE #'S								
TI FILTER	0	1	2	3	4	5	6	7 OF 0-7
ARRAY	15	16	17	18	19	20	21	22 OF 32
NERC PIXEL	5	6	7	8	9	10	11	12 OF 16
CHIP CARRIER	8	44	9	43	10	42	11	41 OF 68
BNC	9	28	10	27	11	26	12	25 OF 36
PREAMP	2	3	6	7	9	10	14	15 OF 16
37D CONNECTOR	36	35	32	31	18	17	13	12 OF 37
D/A CHANNEL	1	2	5	6	8	9	13	14 OF 0-15

RIVERSIDE RESEARCH INSTITUTE

APPENDIX D

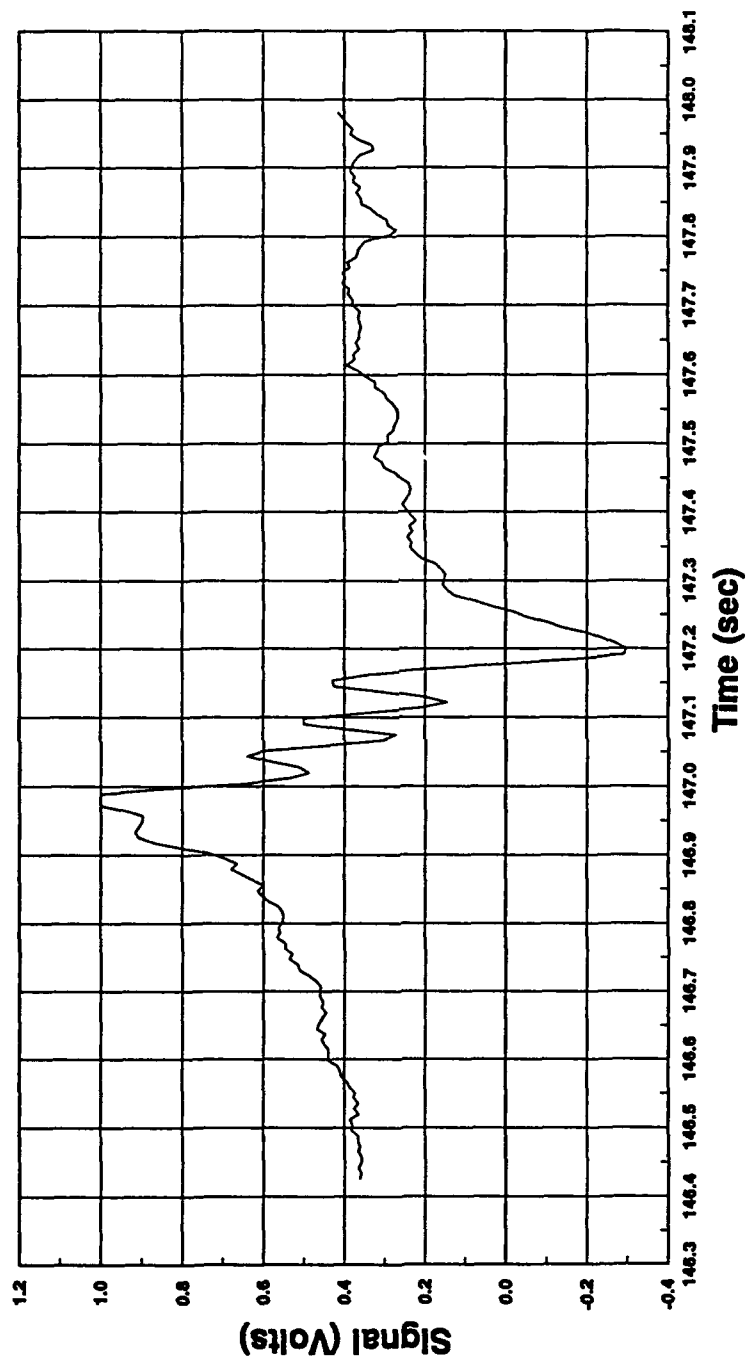
RIVERSIDE RESEARCH INSTITUTE

WEATHER CONDITIONS			
	6/22/92	6/23/92	6/24/92
	60% CLOUDS, 40% SUNSHINE	35% CLOUDS, 65% SUNSHINE	85% CLOUDS, 15% SUNSHINE
TIME	ATMOSPHERIC PRESSURE (mm Hg)		
6:00	760.48	762.25	756.16
12:00	760.73	761.49	755.65
18:00	760.48	758.70	753.36
	TEMPERATURE (°F)/RELATIVE HUMIDITY (%)		
1:00	55/63	55/68	67/58
2:00	54/66	54/74	67/54
3:00	54/68	52/79	68/58
4:00	54/66	53/79	67/67
5:00	52/71	52/79	67/72
6:00	52/71	51/82	67/75
7:00	53/66	54/80	69/72
8:00	56/61	58/71	67/83
9:00	58/57	62/55	68/83
10:00	58/52	66/48	70/78
11:00	57/54	68/38	70/78
12:00	60/47	70/37	71/78
13:00	60/49	71/37	74/65
14:00	63/46	73/36	78/59
15:00	63/44	74/36	79/57
16:00	65/39	75/35	80/53
17:00	66/39	76/32	78/57
18:00	67/39	74/39	73/73
19:00	67/39	74/40	70/75
20:00	65/42	72/47	71/78
21:00	62/49	69/56	69/83

RIVERSIDE RESEARCH INSTITUTE

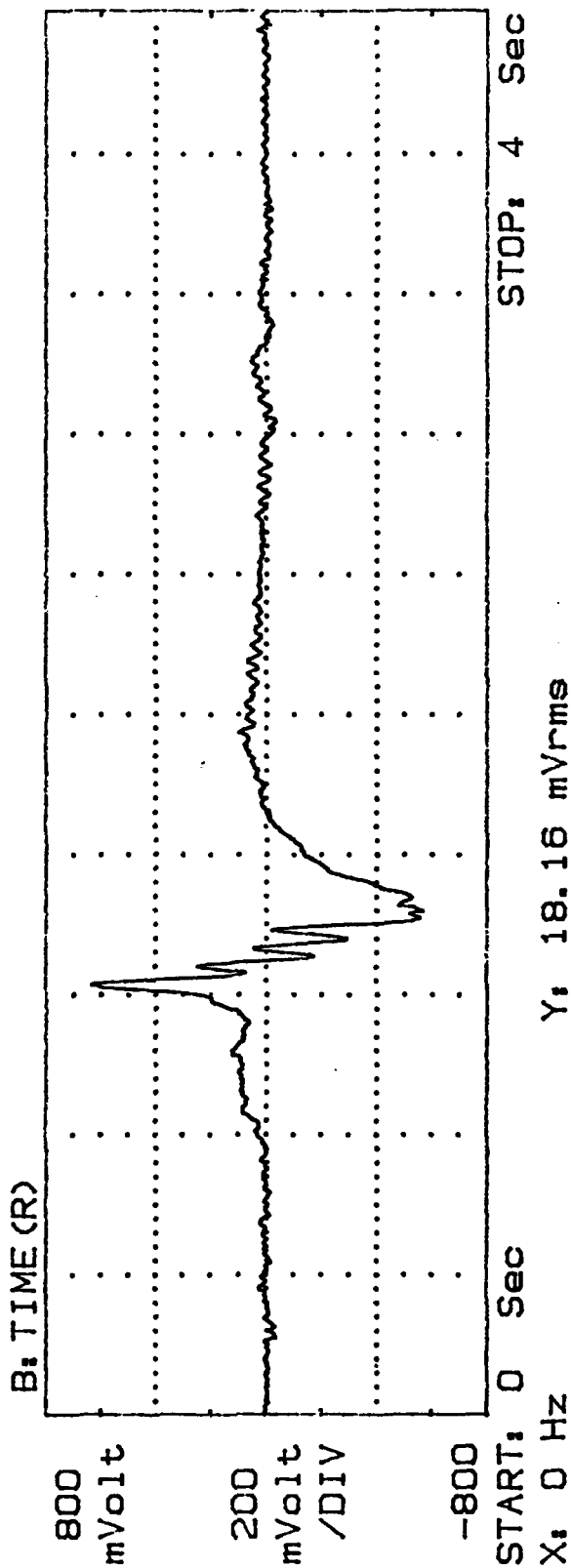
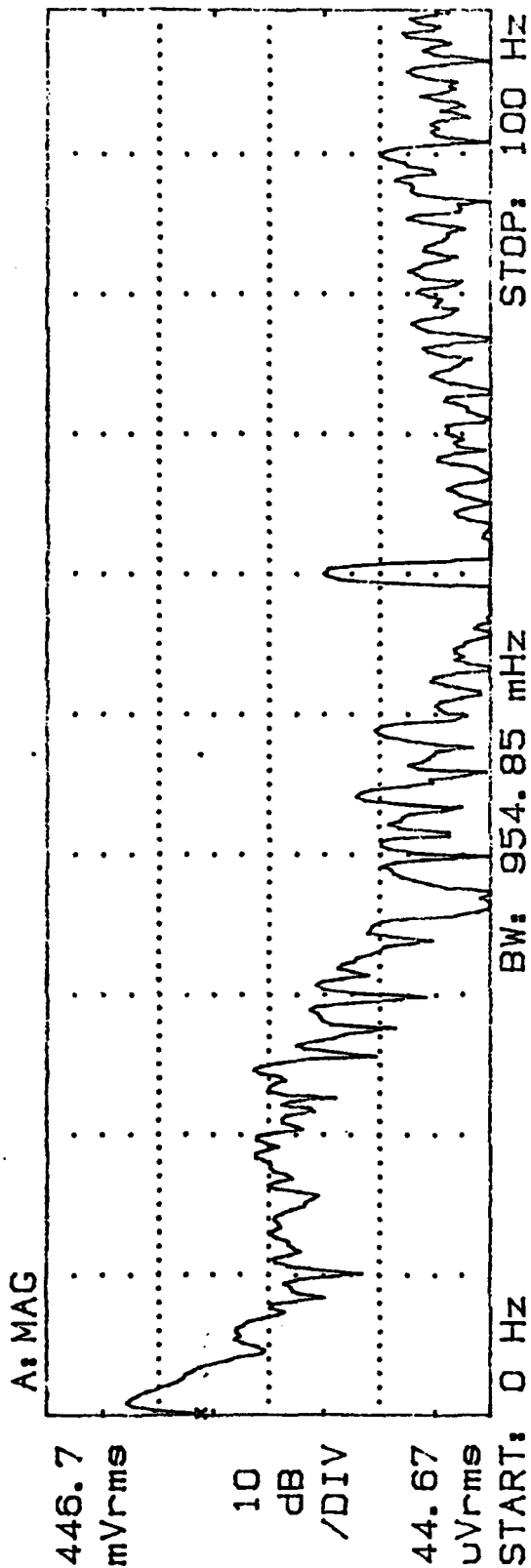
APPENDIX E

Section of Digitized Data File - BASY12.TST



CH 3, 10⁶, FULL PUPIL, 6/22/92
SS 0.093%SEC, 600 C BLACKBODY AT 206 M

RANGE: -7 dBV STATUS: PAUSED



PLOT 1, BASY12, CH 3, 10°, FULL PUPIL, 6/22/92
SS 0.093°/SEC, 600 C BLACKBODY AT 206 M

RANGE: -21 dBV STATUS: PAUSED

A: MAG

89.13
mVrms

10
dB
/DIV

8.913
uVrms

START: 0 Hz

BW: 954.85 mHz

STOP: 100 Hz

B: TIME (R)

200
mVolt

50
mVolt
/DIV

-200

START: 0 Sec

X: 0 Hz

STOP: 4 Sec

Y: 3.110 mVrms

PLOT 2, BASY30, CH 3, 10°, PUPIL 3, 6/22/92
SS 0.093%/SEC, 375 C BLACKBODY AT 206 M

RANGE: -21 dBV STATUS: PAUSED

A: MAG

89.13
mVrms

10
dB
/DIV

8.913
uVrms

START: 0 Hz

BW: 954.85 mHz

STOP: 100 Hz

B: TIME (R)

200
mVolt

50
mVolt
/DIV

-200

START: 0 Sec

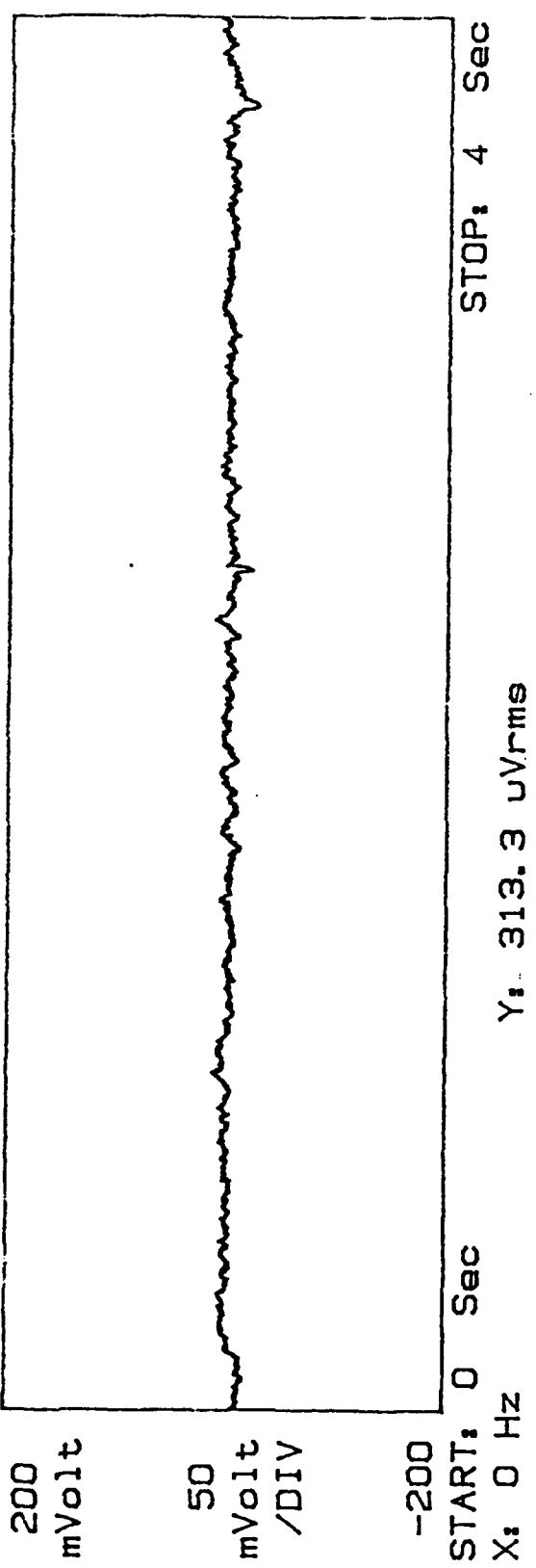
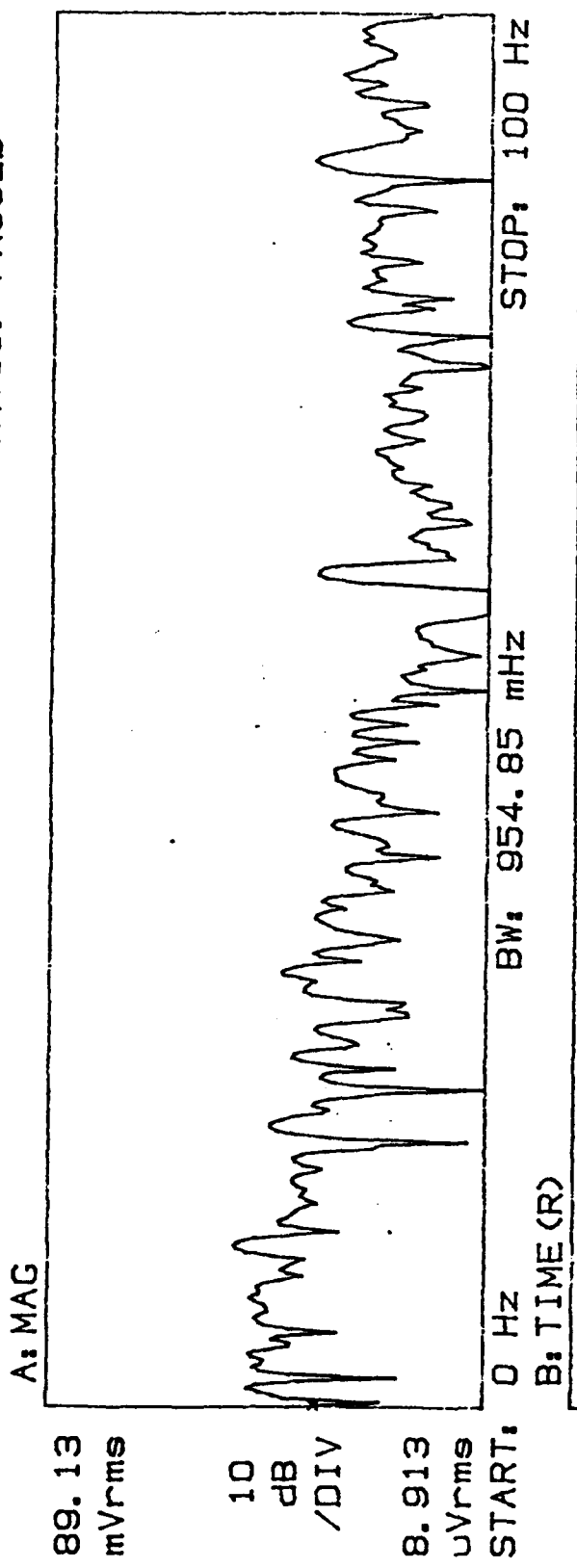
X: 0 Hz

Y: 1.057 mVrms

STOP: 4 Sec

PLOT 3, BASY31, CH 3, 10°, PUPIL 3, 6/22/92
SS 0.093°/SEC

RANGE: -21 dBV STATUS: PAUSED



PLOT 4, BASY32, CH 3, 10°, PUPIL 3, 6/22/92
SS 0.093°/SEC, CIRRO-STRATUS AT > 5 KM

RANGE: -13 dBV STATUS: PAUSED

A: MAG

223.9
mVrms

10
dB
/DIV

22.39
uVrms

START: 0 Hz BW: 954.85 mHz STOP: 100 Hz

B: TIME (R)

400
mVolt

100
mVolt
/DIV

-400

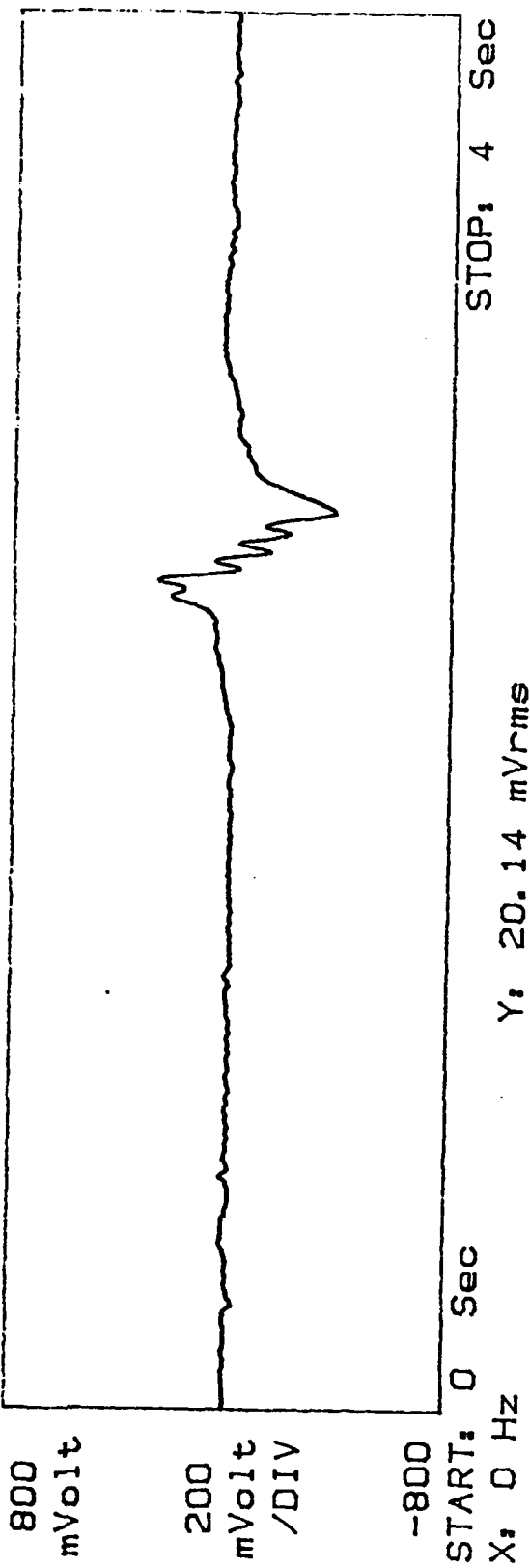
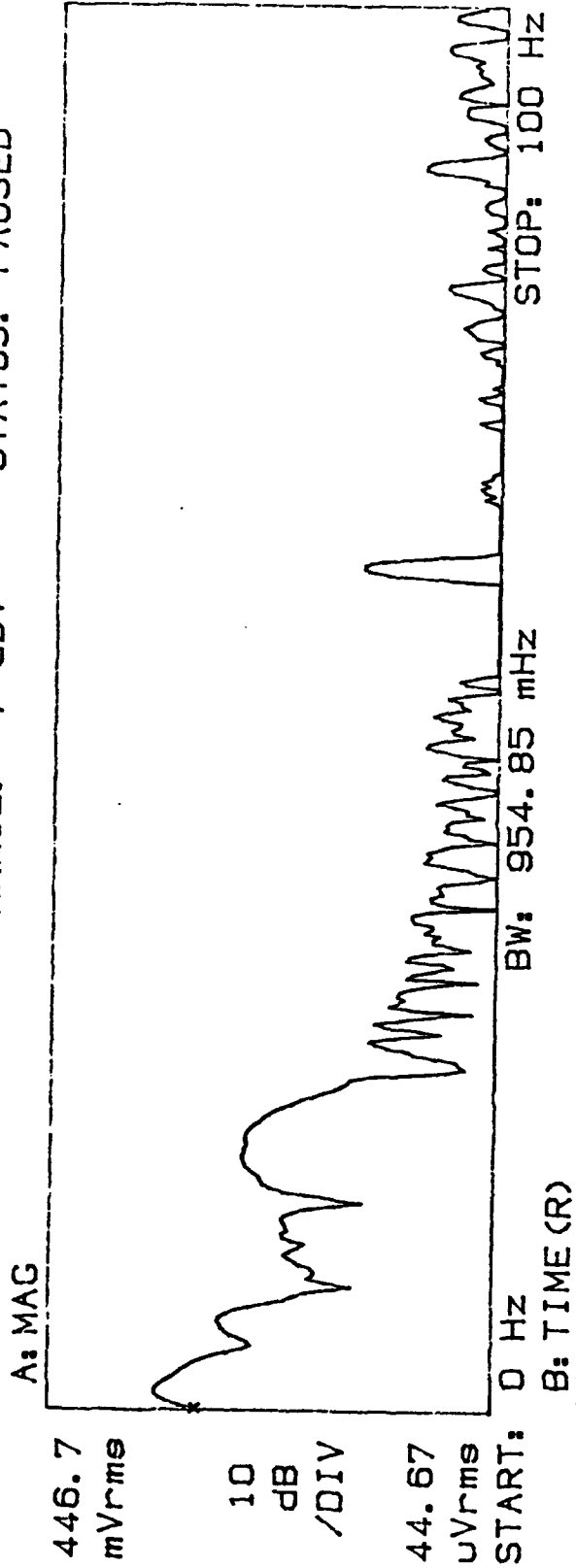
START: 0 Sec
X: 0 Hz

Y: 1.600 mVrms

STOP: 4 Sec

PLOT 5, BASY24, CH 3, 10°, FULL PUPIL, 6/22/92
NON-SCANNING CLOSE TO 375 C BLACKBODY AT 206 M

RANGE: -7 dBV STATUS: PAUSED



PLOT 6, BASY27, CH 3, 10°, FULL PUPIL, 6/22/92
SS 0.093°/SEC, 375 C BLACKBODY AT 206 M

RANGE: -13 dBV STATUS: PAUSED

A: MAG

223.9
mVrms

10
dB
/DIV

22.39
uVrms

START: 0 Hz

BW: 954.85 mHz

STOP: 100 Hz

B: TIME (R)

400
mVolt

100
mVolt
/DIV

-400

START: 0 Sec

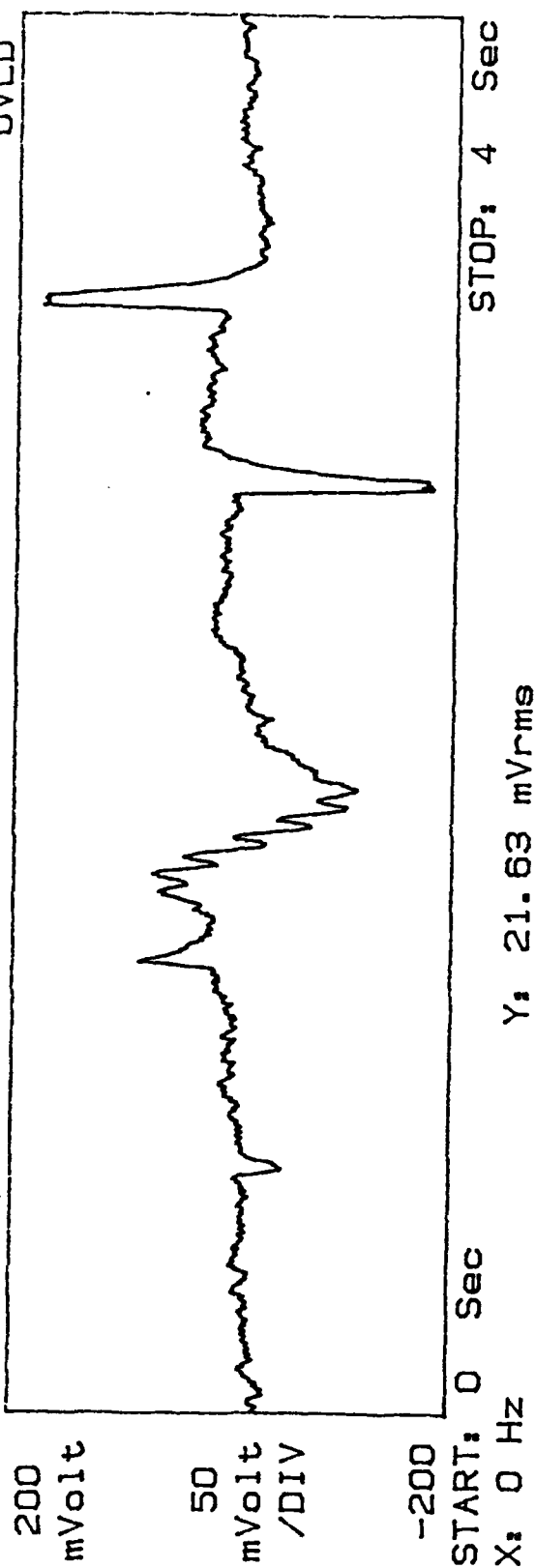
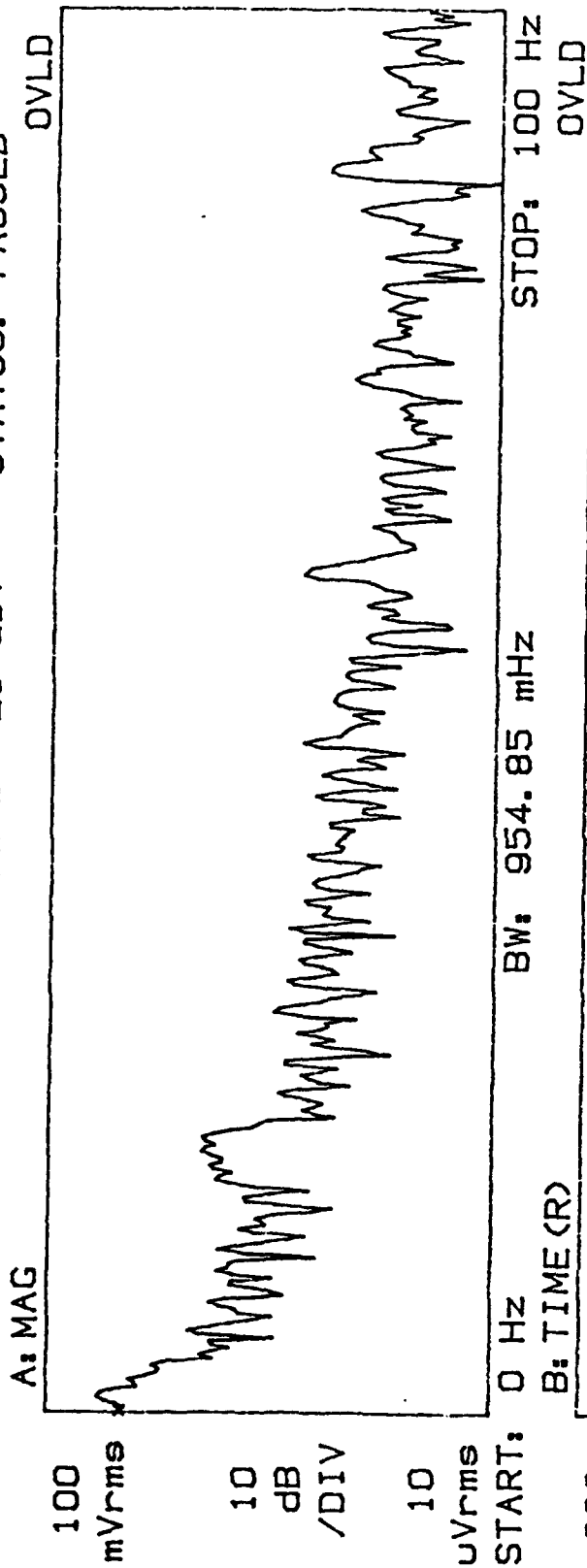
X: 0 Hz

Y: 7.674 mVrms

STOP: 4 Sec

PLOT 7, BASY29, CH 3, 10⁶, PUPIL 3, 6/22/92
SS 0.093%/SEC, 375 C BLACKBODY AT 206 M

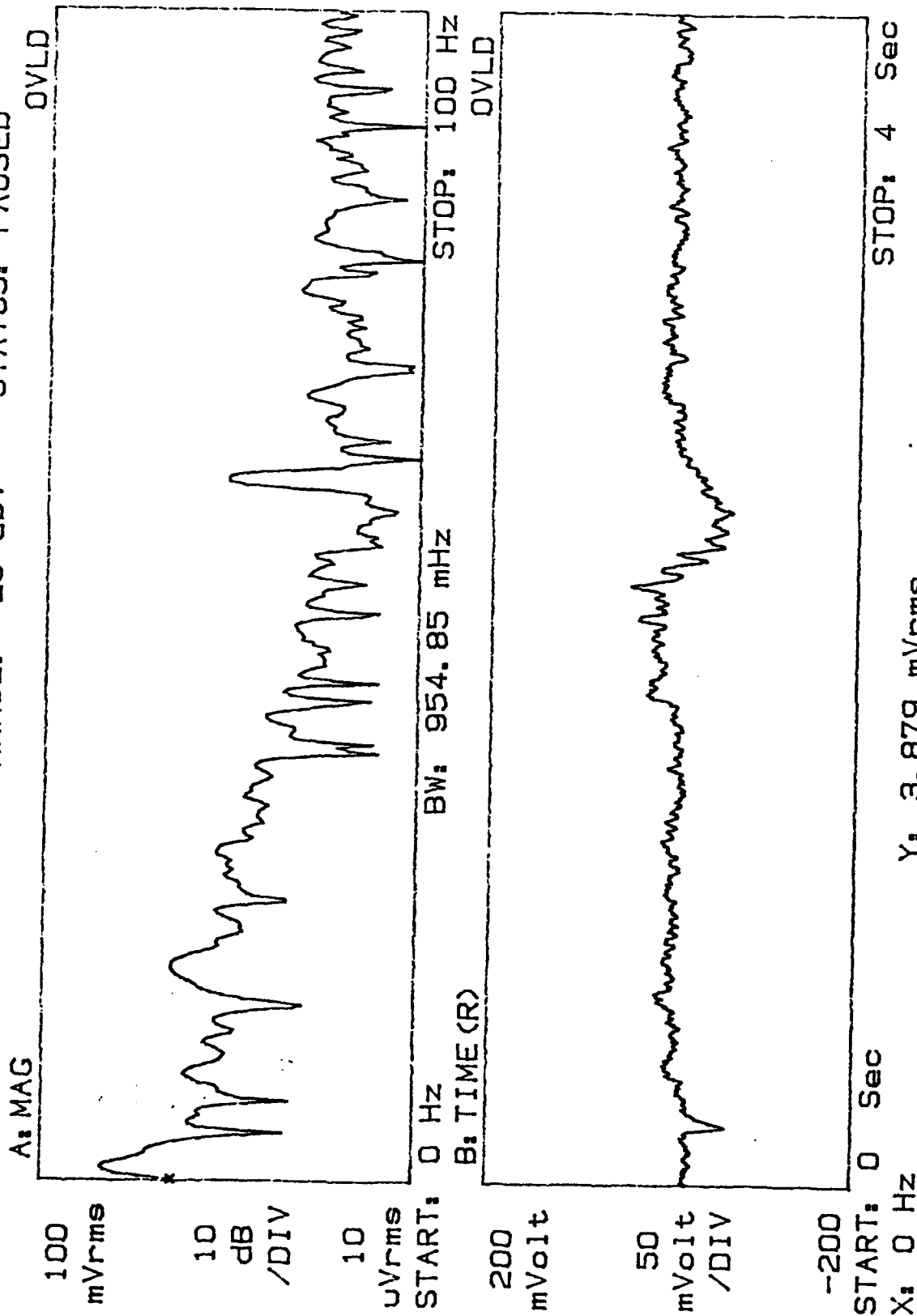
RANGE: -20 dBV STATUS: PAUSED



Y: 21.63 mVrms

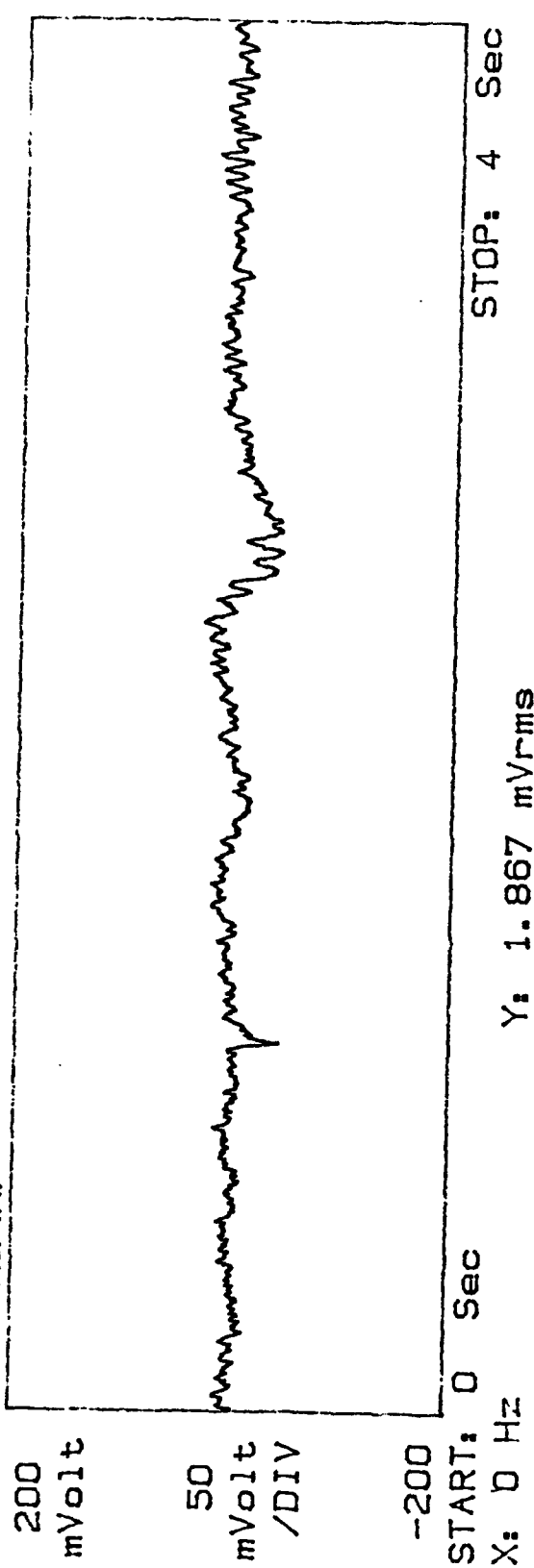
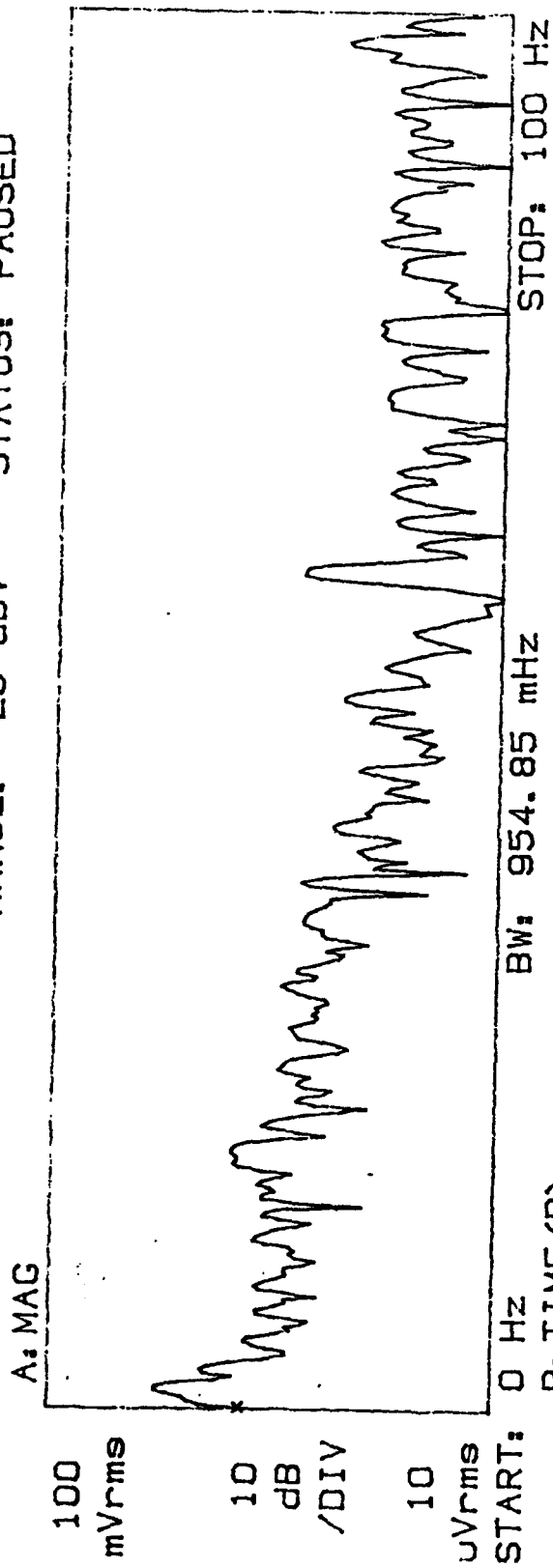
PLOT 8, BASY21, CH 3, 10⁶, PUPIL 3, 6/22/92
SS 0.093⁰/SEC, 500 C BLACKBODY AT 206 M

RANGE: -20 dBV STATUS: PAUSED



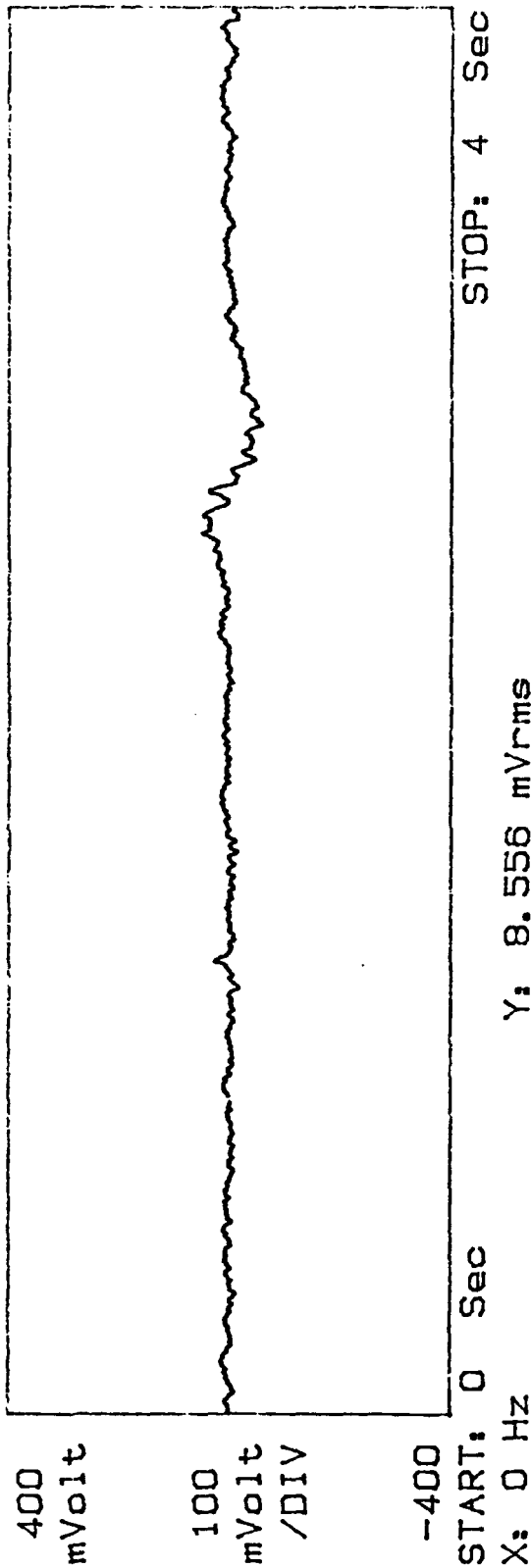
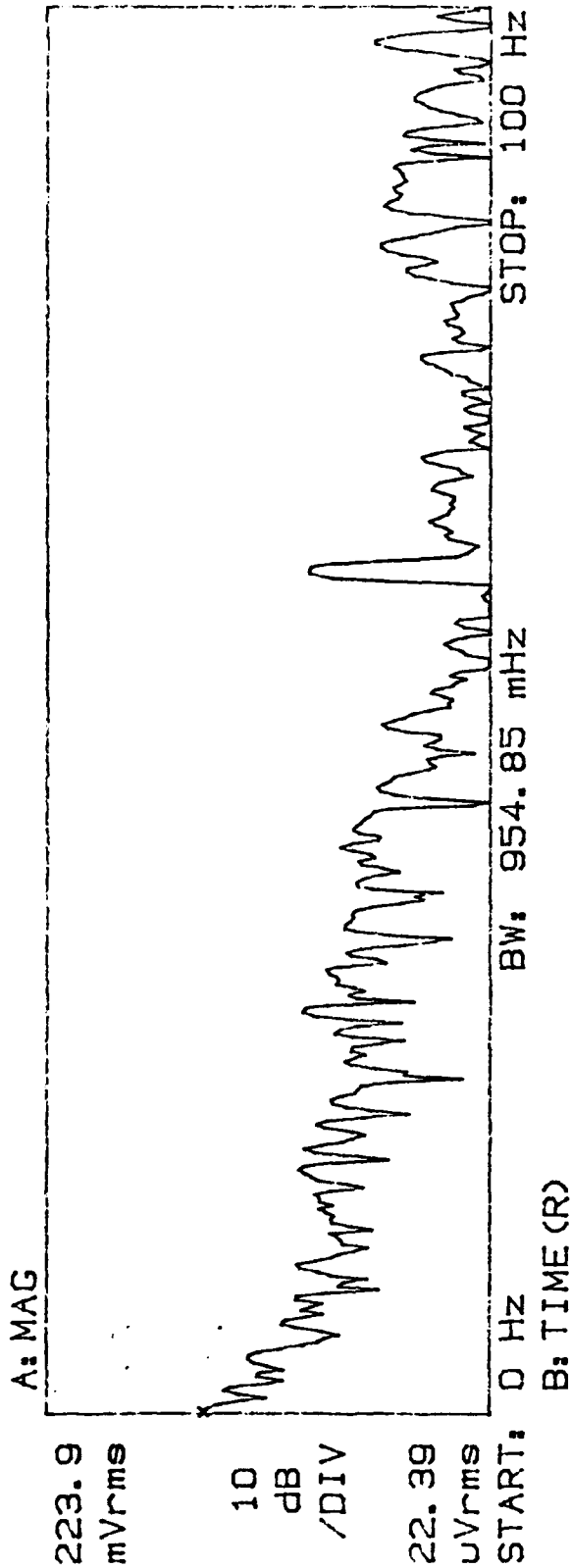
PLOT 9, BASY18, CH 3, 10°, PUPIL 2, 6/22/92
SS 0.093%/SEC, 600 C BLACKBODY AT 206 M

RANGE: -20 dBV STATUS: PAUSED



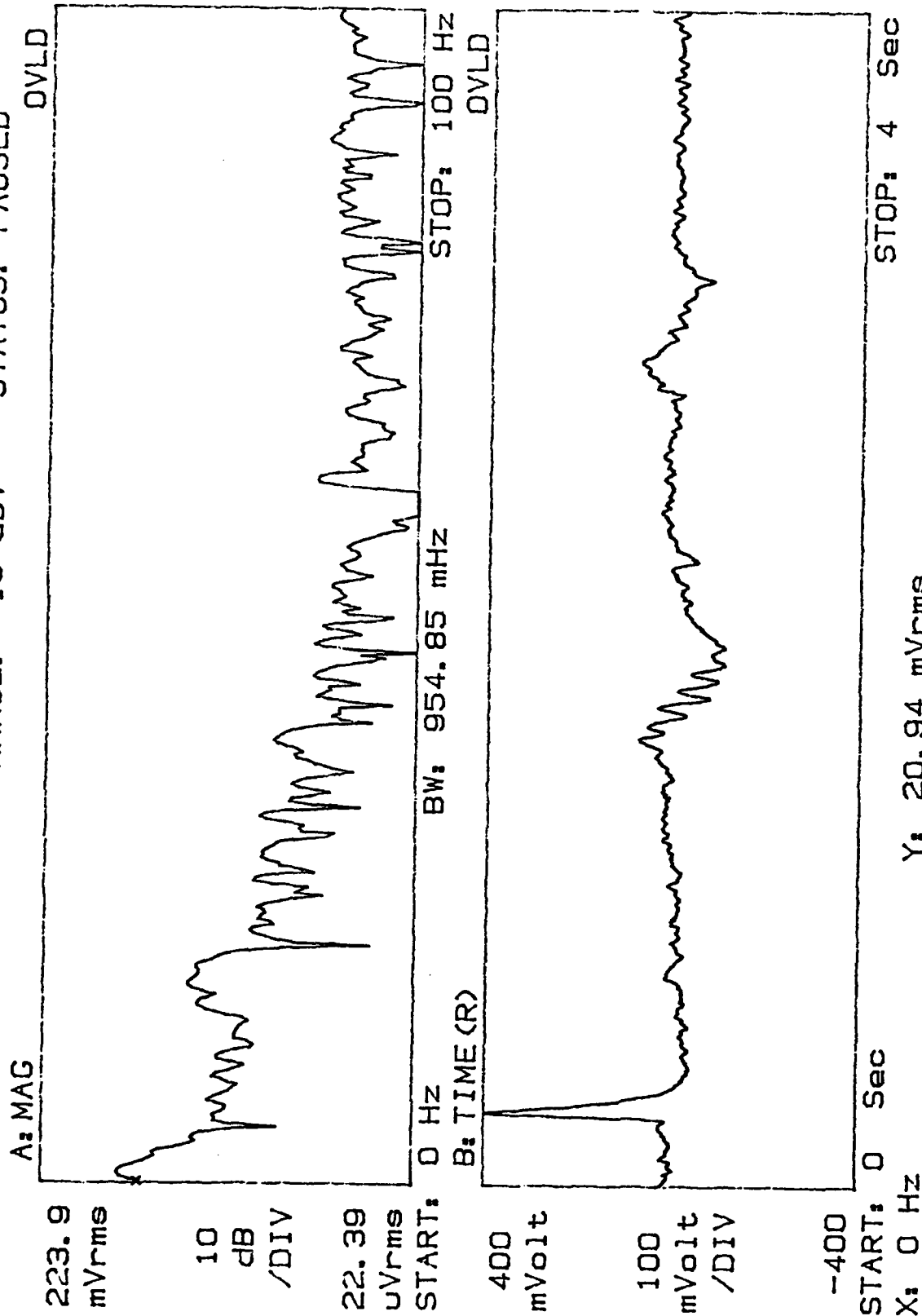
PLOT 10, BASY19, 20, SIMILAR, CH 3, PUPIL 2, 6/22/92
SS 0.093°/SEC, 600 C BLACKBODY AT 206 M

RANGE: -13 dBV STATUS: PAUSED

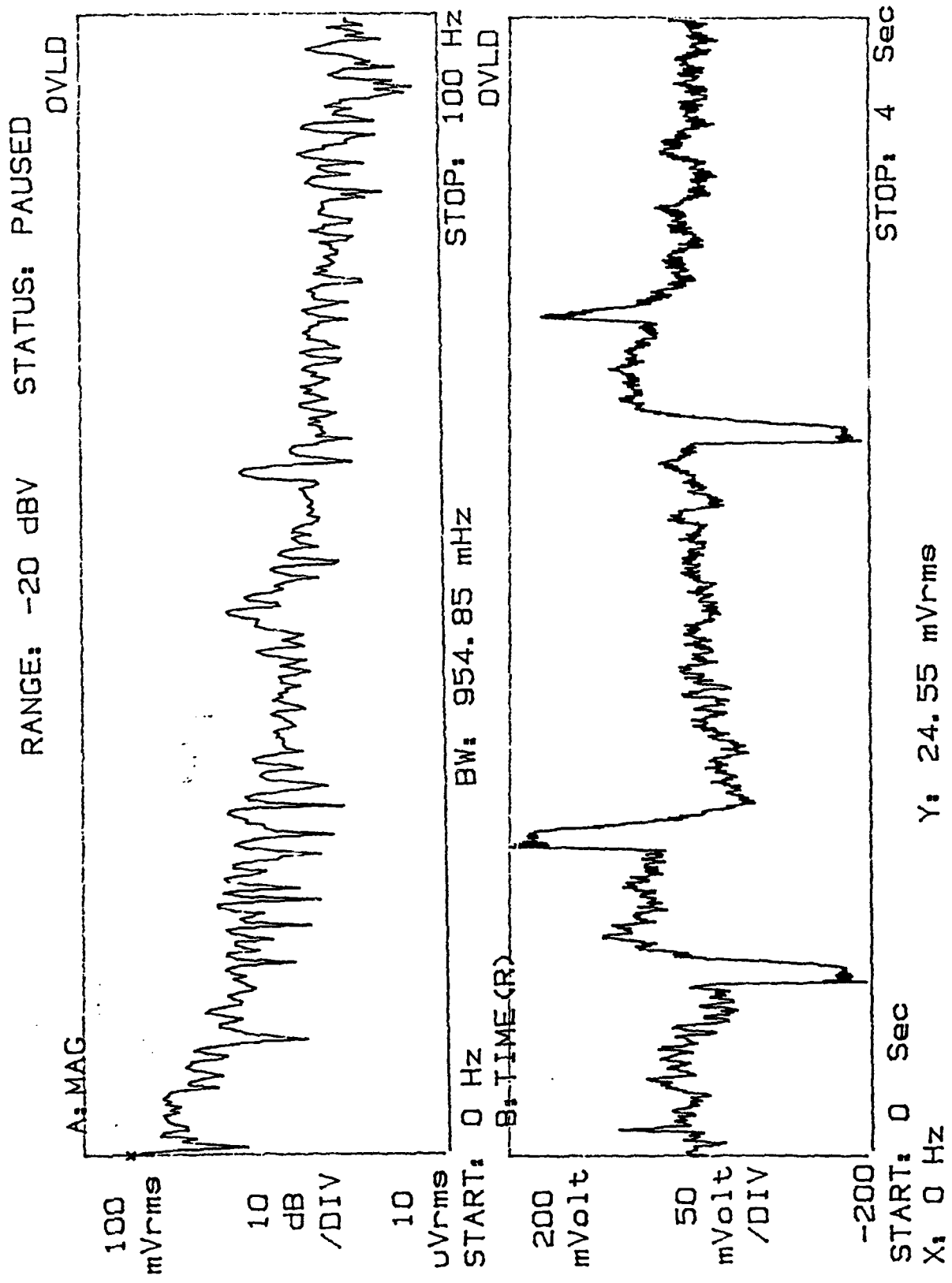


PLOT 11, BASY17, CH 3, 10°, PUPIL 2, 6/22/92
SS 0.093°/SEC, 600 C BLACKBODY AT 206 M.

RANGE: -13 dBV STATUS: PAUSED

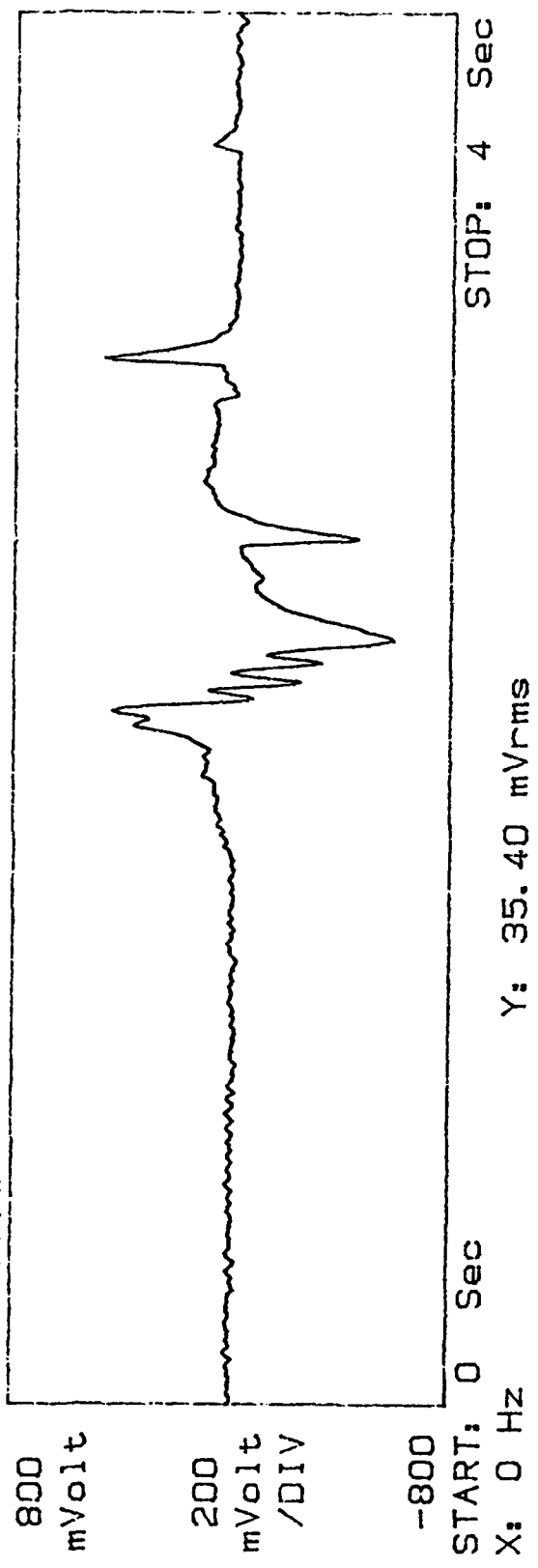
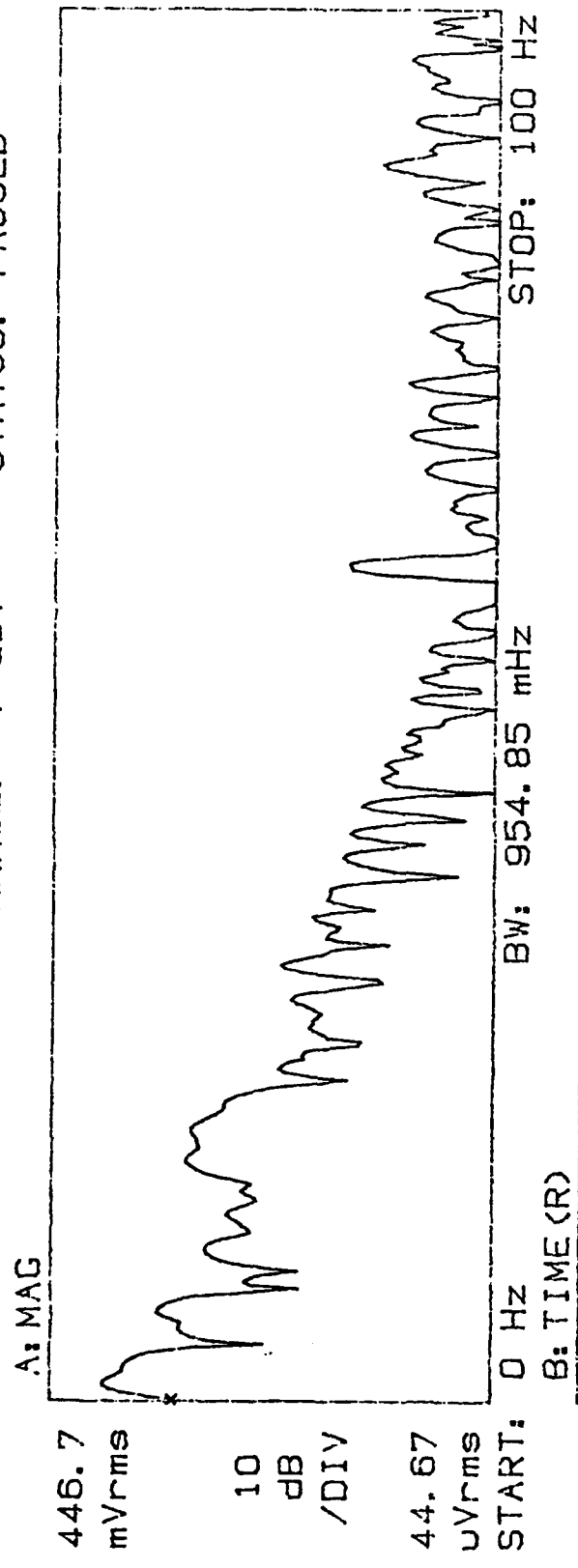


PLOT 12, BASY16, CH 3, 10⁶, PUPIL 3, 6/22/92
 SS 0.093%/SEC, 600 C BLACKBODY AT 206 M



PLOT 13, NO FILE, CH 3, 10°, PUPIL 2, 6/22/92
SS 0.093°/SEC, APERTURE COVERED, TYPICAL TRANSIENTS

RANGE: -7 dBV STATUS: PAUSED



PLOT 14, BASY23, CH 3, FULL PUPIL, 6/22/92
SS 0.093°/SEC 500 C BLACKBODY AT 206 M

RANGE: -13 dBV STATUS: PAUSED

A: MAG

223.9
mVrms

10
dB
/DIV

22.39
uVrms

START: 0 Hz

BW: 954.85 mHz

STOP: 100 Hz

B: TIME (R)

400
mVolt

100
mVolt
/DIV

-400

START: 0 Sec

X: 0 Hz

Y: 516.4 uVrms

STOP: 4 Sec

PLOT 15, BASZ25, CH 3, 10°, PUPIL 2, 6/22/92
NON-SCANNING, GRASS AT 206 M

RANGE: -7 dBV STATUS: PAUSED

A: MAG

446.7
mVrms

10
dB
/DIV

44.67
uVrms

START:

0 Hz

B: TIME (R)

BW: 954.85 mHz

STOP: 100 Hz

800
mVolt

200
mVolt
/DIV

-800

START: 0 Sec

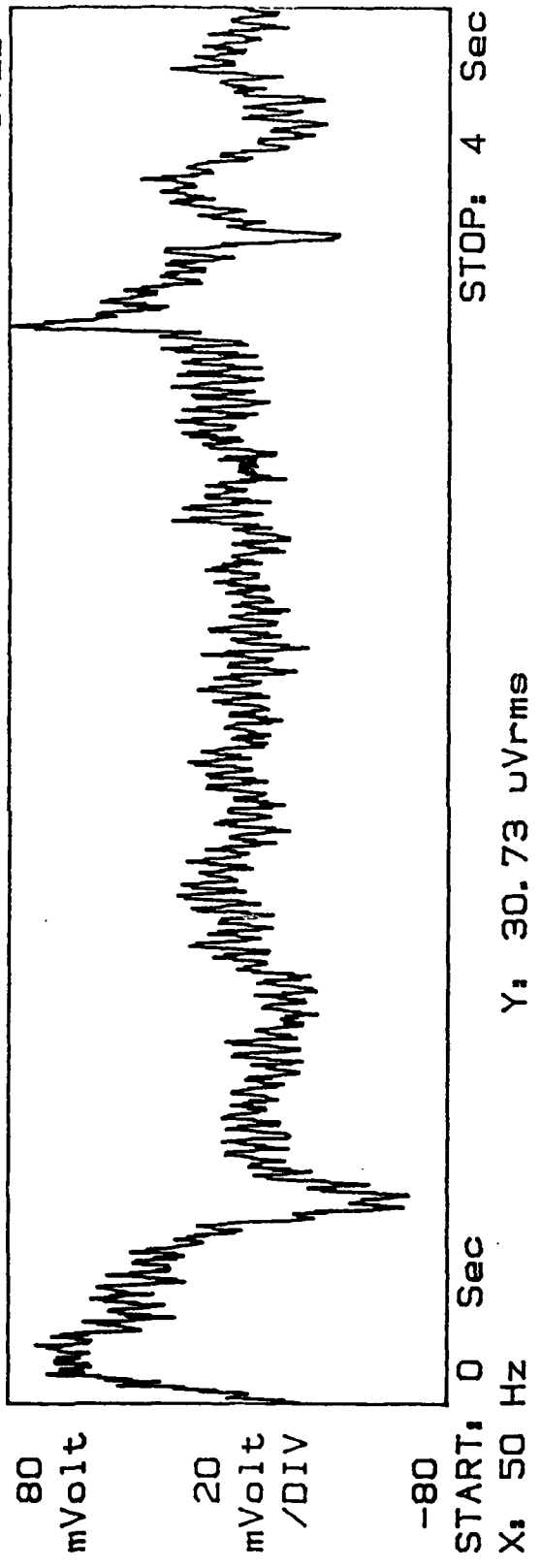
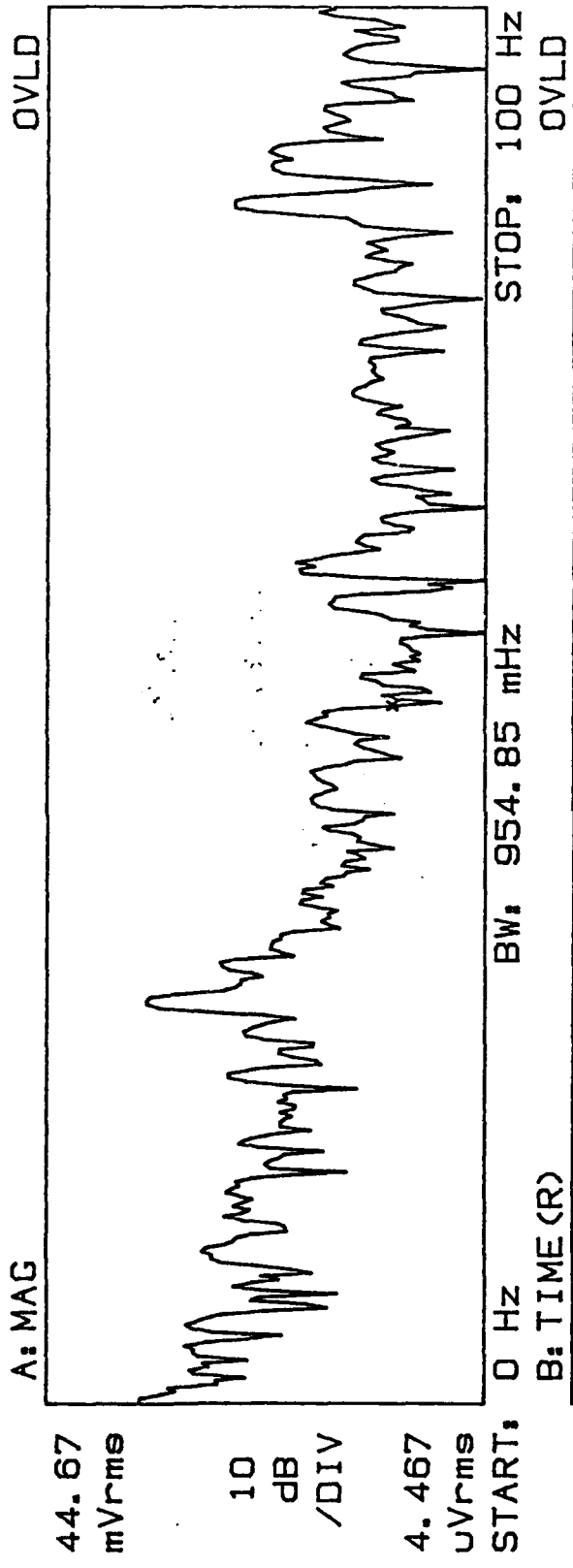
X: 0 Hz

Y: 25.73 mVrms

STOP: 4 Sec

PLOT 16, NO FILE, CH 3, 10°, PUPIL 2, 6/22/92
NON-SCANNING, TYPICAL NOISE SPIKE

RANGE: -27 dBV STATUS: PAUSED



PLOT 17, BASZ8, CH 3, 10°, PUPIL 2, 6/23/92
NON-SCANNING, -20° AZ, +15° EL

RANGE: -27 dBV STATUS: PAUSED

CVLD

A: MAG

44.67
mVrms

:0
dB
/DIV

4.467
uVrms

START: 0 Hz

BW: 954.85 MHz

STOP: 100 Hz

B: TIME (R)

OVLD

80
mVolt

20
mVolt
/DIV

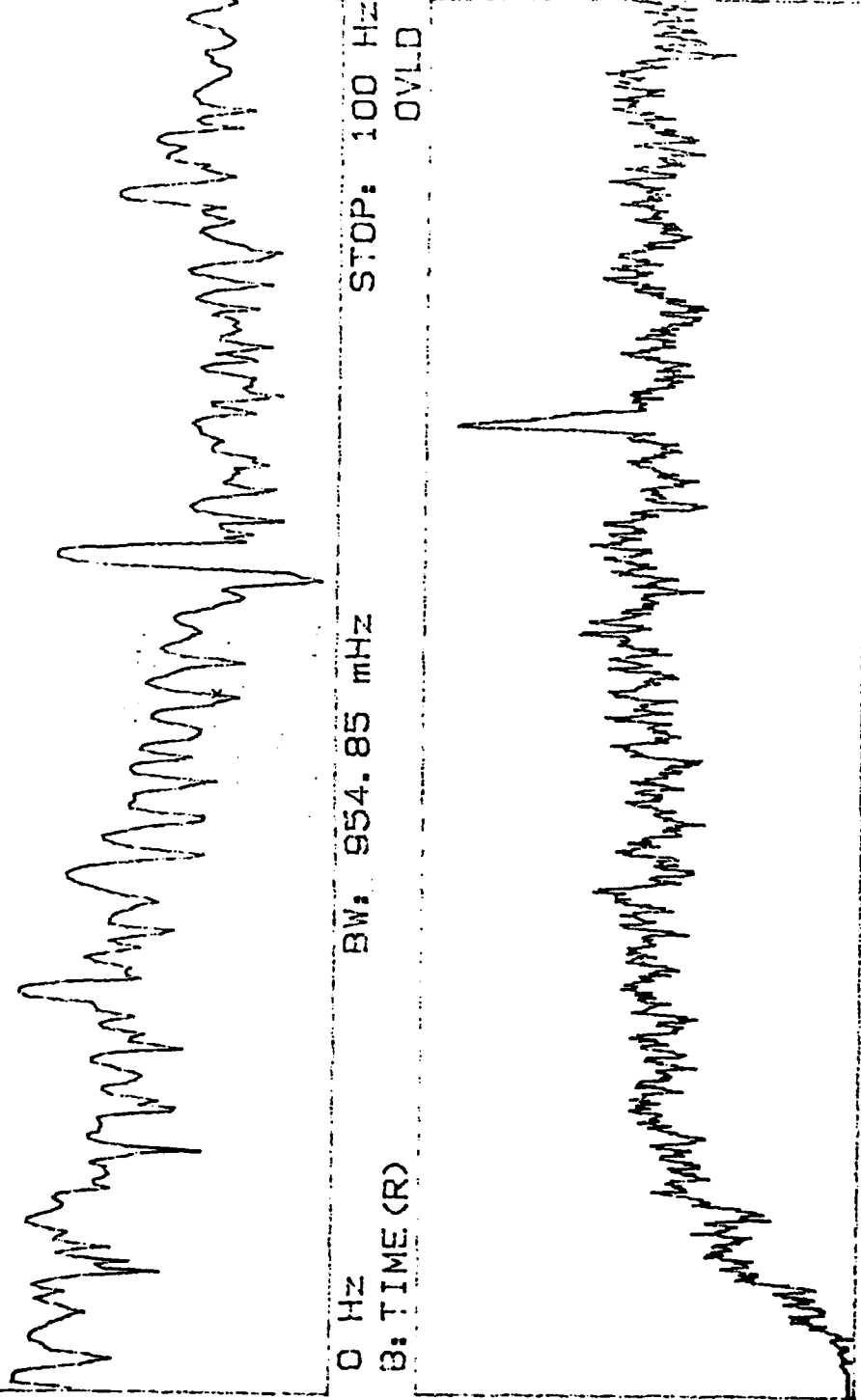
-80

START: 0 Sec

X: 50 Hz

Y: 54.04 uVrms

STOP: 4 Sec



PLOT 18, BASZ7, CH 3, 10°, PUPIL 2, 6/23/92
SS 0.093°/SEC

RANGE: -20 dBV STATUS: PAUSED

A: MAG

100
mVrms

10
dB
/DIV

10
uVrms

START: 0 Hz

BW: 954.85 MHz

STOP: 100 Hz

B: TIME (R)

200
mVolt

50
mVolt
/DIV

-200

START: 0 Sec

X: 50 Hz

Y: 473.2 uVrms

STOP: 4 Sec

PLOT 19, BASZ4, CH 3, 10°, PUPIL 2, 6/23/92
SS 0.093°/SEC, BUILDING AT 200 M

RANGE: -20 dBV STATUS: PAUSED

A: MAG

100
mVrms

10
dB
/DIV

10
uVrms

START:

0 Hz

BW: 954.85 mHz

STOP: 100 Hz

B: TIME (R)

200
mVolt

50
mVolt
/DIV

-200

START:

0 Sec

X: 50 Hz

Y: 160.0 uVrms

STOP: 4 Sec

PLOT 20, NO FILE, CH 3, PUPIL 2, 6/23/92
SS 0.093°/SEC, RELATIVELY NOISLESS

RANGE: -33 dBV STATUS: PAUSED

A: MAG

OVLD

22.39
mVrms

10
dB
/DIV

2.239
uVrms

START: 0 Hz

BW: 954.85 mHz

STOP: 100 Hz

B: TIME(R)

OVLD

40
mVolt

10
mVolt
/DIV

-40

START: 0 Sec

X: 50 Hz

STOP: 4 Sec

Y: 59.63 uVrms

PLOT 21, BASZ5, CH 3, 10⁶, PUPIL 2, 6/23/92
SS 0.093°/SEC, RELATIVELY NOISELESS

RANGE: -27 dBV STATUS: PAUSED

A: MAG

44.67
mVrms

10
dB
/DIV

4.467
uVrms

START: 0 Hz

BW: 954.85 MHz

STOP: 100 Hz

B: TIME (R)

80
mVolt

20
mVolt
/DIV

-80

START: 0 Sec

X: 50 Hz

Y: 84.63 uVrms

STOP: 4 Sec

PLOT 22, BASZ6, CH 3, 10°, PUPIL 2, 6/23/92
SS 0.093°/SEC, TOP-LIT CUMULOUS

RANGE: -27 dBV STATUS: PAUSED

A: MAG

44.67
mVrms

10
dB
/DIV

4.467
uVrms

START:

0 Hz

BW: 954.85 mHz

STOP: 100 Hz

B: TIME (R)

80
mVolt

20
mVolt
/DIV

-80

START: 0 Sec

X: 50 Hz

Y: 174.0 uVrms

STOP: 4 Sec

PLOT 23, BASZ5, CH 3, 10°, PUPIL 2, 6/23/92
SS 0.093°/SEC, TOP-LIT CUMULOUS

RANGE: -20 dBV STATUS: PAUSED

DVLD

A: MAG

100

mVrms

10

dB

/DIV

10

uVrms

START: 0 Hz

BW: 954.85 mHz

STOP: 100 Hz

B: TIME (R)

DVLD

200

mVolt

50

mVolt

/DIV

-200

START: 0 Sec

X: 50 Hz

STOP: 4 Sec

Y: 273.5 uVrms

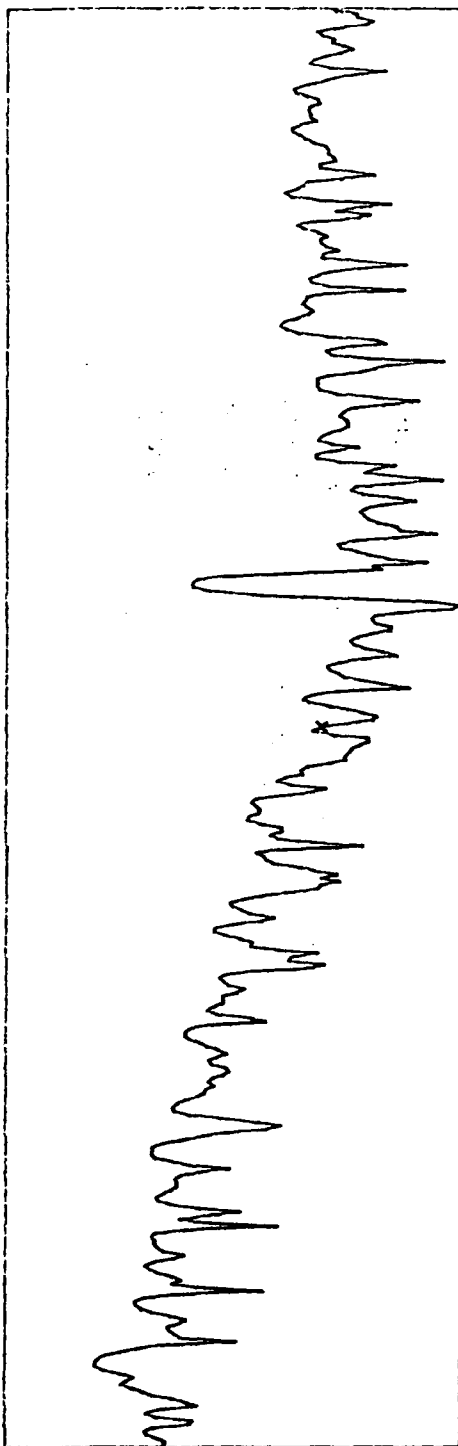
PLOT 24, BASZA, CH 3, PUPIL 2, 6/23/92

SS 0.093°/SEC

RELATIVELY NOISY

RANGE: -20 dBV STATUS: PAUSED

A: MAG

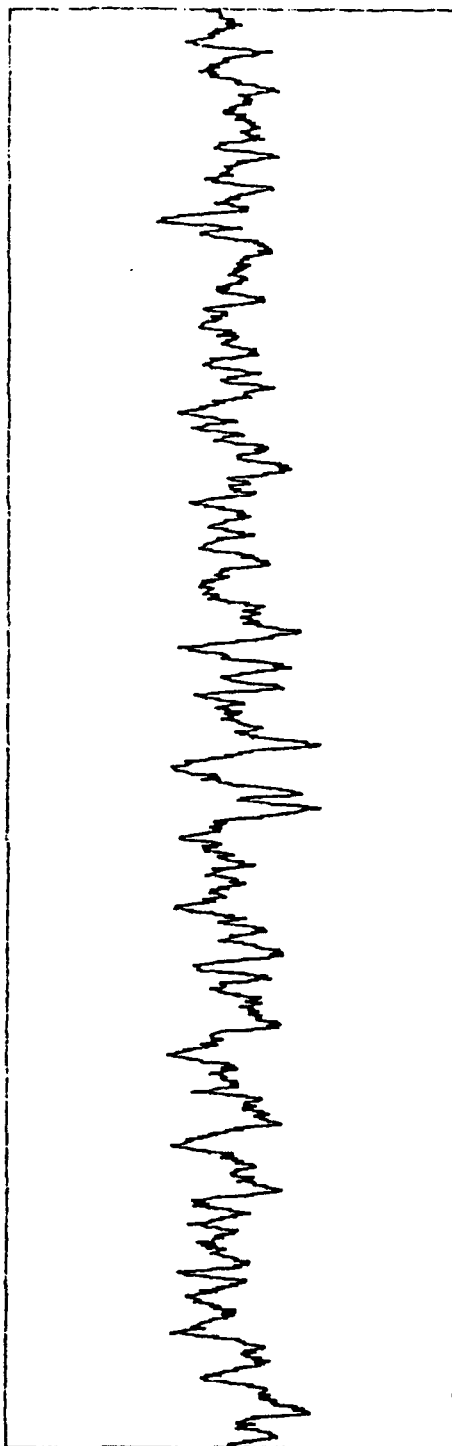


STOP: 100 Hz

BW: 954.85 mHz

START: 0 Hz

B: TIME (R)



STOP: 4 Sec

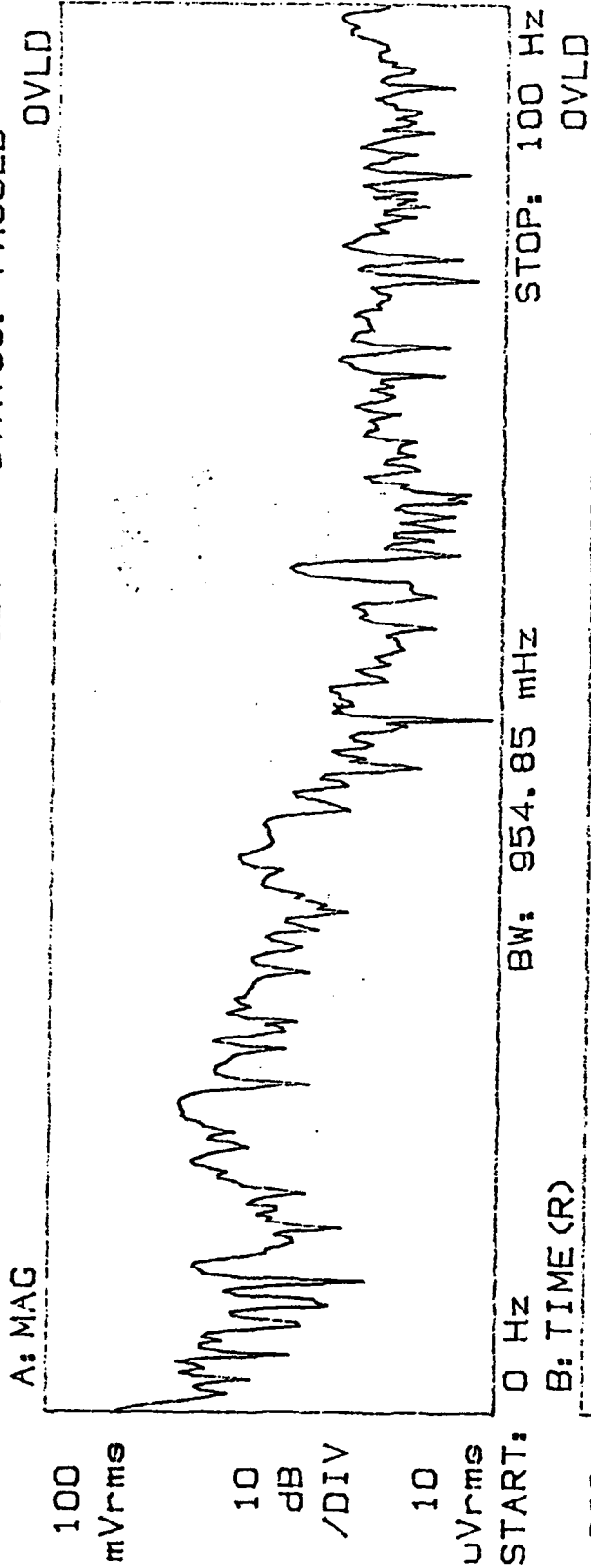
START: 0 Sec

X: 50 Hz

Y: 173.7 uVrms

PLOT 25, BASZ0, CH 3, 10°, PUPIL 2, 6/23/92
NON-SCANNING, APERTURE COVERED
TYPICAL NOISE

RANGE: -20 dBV STATUS: PAUSED



PLOT 26, BASZ1, CH 3, 10°, PUPIL 2, 6/23/92
NON-SCANNING, APERTURE COVERED
TYPICAL NOISE SPIKE